Analysis of metrics for human detection behind walls using experimental 3-D synthetic aperture radar imagery

Brigitte Chan
Pascale Sévigny
David J. DiFilippo
DRDC – Ottawa Research Centre

Defence Research and Development Canada

Scientific Report
DRDC-RDDC-2014-R140
December 2014

Abstract

Defence Research and Development Canada (DRDC) has been investigating 3-D through wall synthetic aperture radar (SAR) imaging from an experimental L-band through-wall SAR prototype. Tools and algorithms are being developed to exploit the resulting 3-D imagery. In this report, a comprehensive study of the characteristics of human target signatures behind three different wall structures is presented using 3-D SAR data. An analysis of the human target signature in different poses behind a drywall, a cinder block wall, and a brick/cinder block wall is provided. The aim of this investigation is to determine different quantitative features that could be used as potential discriminants. A comprehensive study of 3-D human target signature metrics behind drywall is also provided. The aim of this study is to identify features for discrimination of the human target from other similar features in an empty scene including the wall signature, potential ghosts, and clutter and multipath. Several metrics were investigated as potential discriminants and six were identified as good candidates. Based on this study, no single metric could be used to fully discriminate the human targets from all others. A combination of at least three different metrics is required to achieve this. These metrics can now be implemented in an automatic human target detection algorithm for analysis.

Significance to defence and security

This study of metrics for discriminating human targets from other sources behind walls will allow the next phase of automatic human target detection inside buildings to be developed. This situational awareness capability can be invaluable to the military working in a highly cluttered urban environment, where data can be collected and processed at a safe stand-off position.

Résumé

Recherche et développement pour la défense Canada (RDDC) étudie l'imagerie 3D par radar à synthèse d'ouverture (RSO) à travers les murs à l'aide d'un prototype expérimental de RSO à travers les murs en bande L. Des outils et des algorithmes sont en développement en vue d'exploiter les images 3D ainsi obtenues. Le rapport présente les données RSO 3D d'une étude approfondie menée sur les caractéristiques des signatures de cibles humaines derrière trois structures murales différentes. Il comporte également l'analyse d'une signature de cible humaine selon différentes positions, derrière une cloison sèche, un mur en bloc de béton d'escarbilles et un mur en briques et en bloc de béton d'escarbilles. L'étude vise à déterminer différentes caractéristiques quantitatives qui pourraient servir de discriminants potentiels. Le rapport comporte aussi une étude approfondie menée sur les paramètres des signatures de cibles humaines 3D derrière une cloison sèche. Cette étude vise à déterminer des caractéristiques permettant de discerner une cible humaine parmi d'autres caractéristiques similaires dans une scène vide, notamment la signature murale, les effets d'échos potentiels, le fouillis et les trajets multiples. De tous les paramètres examinés en tant que discriminants potentiels, six ont été retenus. D'après l'étude, il est impossible de discerner parfaitement les cibles humaines parmi d'autres cibles à l'aide d'un seul paramètre. En effet, une combinaison d'au moins trois paramètres différents est nécessaire. Il est désormais possible de mettre en œuvre ces paramètres dans un algorithme de détection de cibles humaines automatique aux fins d'analyses.

Importance pour la défense et la sécurité

Grâce à l'étude des paramètres qui permettent de discerner une cible humaine parmi d'autres sources derrière des murs, RDDC pourra commencer le développement de la détection de cibles humaines automatique au sein de bâtiments. Cette capacité de connaissance de la situation peut être inestimable pour les militaires qui travaillent dans un environnement urbain fort encombré où les données peuvent être acquises et traitées depuis une position à distance de sécurité.

Table of contents

List of figures

List of tables

Acknowledgements

We are grateful to Janice Lang, official DRDC Ottawa photographer, and to Michel Vigneault, official DRDC Valcartier photographer, for all photographs in this technical memorandum. We are also grateful to Jonathan Fournier who provided us with the ground truth to support our analysis and to the engineer and technicians, Tony Laneve, Pietro Reitano, Norm Reed, and Casey Potter for their invaluable expertise during the data collection trials.

1 Introduction

The analysis of through-wall radar imagery is an emerging research area [1]. Research has led to commercial products where devices are stationary during scanning [2]. Researchers continue to investigate through-wall radar technology using different systems and imaging techniques, for example, [9]. The capability to capture high-resolution 3-D through-wall radar imagery data while moving at a stand-off distance is not prominent in the literature. Development of a prototype 3-D through-wall synthetic aperture radar (SAR) system with this capability is currently underway [13]. The intent is to map out building wall layouts and to detect targets of interest behind walls such as humans, arms caches, and furniture. This situational awareness capability can be invaluable to the military working in an urban environment. The experimental SAR radar testbed operates in the L-band. The side-looking radar is truck-mounted with data collected as the vehicle is driven past the front of a building of interest. The system operates over a 1.86 GHz bandwidth between 0.85 and 2.71 GHz. It has two transmit and eight receive antennas [14]. The radar system is shown in Figure 1. It is complemented by a light detection and ranging system (LIDAR) and a positioning system, both truck-mounted as well, as seen in the figure. The LIDAR provides high resolution images of the exterior of a building. It adds another layer of information to help with the interpretation of the SAR data. The positioning system is used for motion compensation as well as to provide an accurate point of reference.

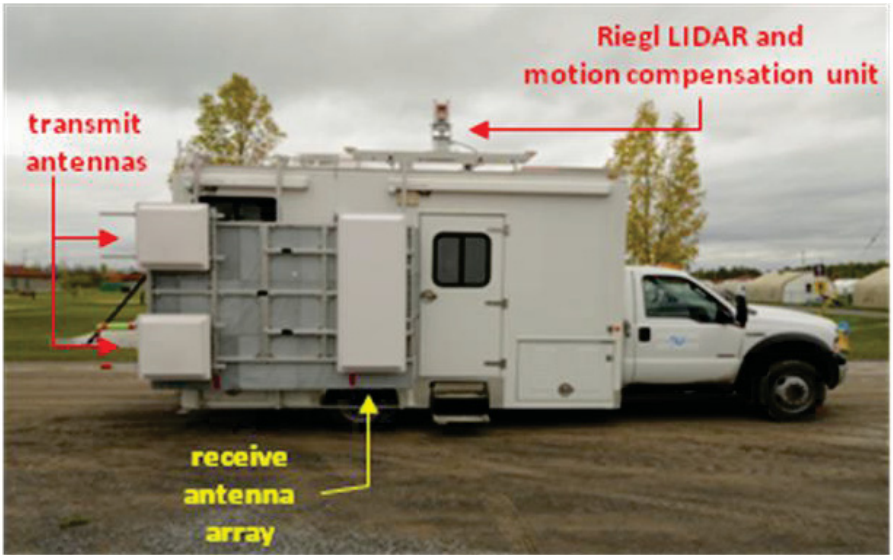

***Figure 1**: 3-D through-wall SAR system.*

The SAR and LIDAR data are collected while the truck moves along the SAR path parallel to the building of interest. It is typically located approximately 10 meters from the front wall if the road structure allows. The azimuth direction is parallel to the SAR path while the range direction is perpendicular to it. Offline, following acquisition, the raw SAR data are pre-processed for proper formatting and motion compensation, pulse-compressed in range, and then a back projection algorithm is applied to form the SAR image [15].

A set of trials was conducted in 2012 in Valcartier. In this report, 3-D free space and behind wall data acquired during the 2012 Trials were used to study the characteristics of free-space and through-wall human target signatures using 3-D SAR data from the radar system. A summary of all scenes and targets is provided in Annex A. An analysis of the human target signature in different poses is provided. Targets used in this investigation include a human in a standing position, a human standing with arms stretched, a human kneeling, a human holding an AK47 in a vertical position, a human holding an AK47 in an angled position, and a human sitting in a chair, all at approximately 8–12m in range with reference to the truck-mounted radar system at closest approach. Buildings used in this investigation include the Troop Shelter (drywall), the Bar (cinder block), and Building 502 (cinder block with a layer of brick in front), all located at DRDC in Valcartier, Quebec. Photographs of the target positions are presented in Figure 2.

(a) (b) (c) (d) (e) (f)

***Figure 2**: Photographs of the targets: (a) human standing arms down; (b) human standing arms stretched; (c) human kneeling; (d) human standing with AK47 in angled position; (e) human standing with AK47 in vertical position; and (f) human sitting in chair.*

In this report, a comprehensive study of 3-D human target signature metrics behind drywall is also provided. The aim of this study is to identify features for discrimination of the human target inside a building from other similar detections in an empty scene including the wall signature, potential ghosts, and clutter and multipath. Several metrics were investigated as potential discriminants.

Free space signatures of the human in various poses are described in Section 2. In Section 3, signatures of the human standing in various poses behind different wall structures, including drywall, cinder block, and a brick/cinder block wall are described. In Section 4, potential discriminants analyzed for human target detection behind walls are presented. An analysis of metrics applied to wall features and other clutter/multipath features behind a drywall is presented in Section 5. In Section 6, conclusions and future research are presented.

2 Human target signatures in free space

2.1 Viewing of the SAR data

Targets of interest in 3-D SAR data are currently detected manually. To do this, the 3-D SAR data are typically displayed in three 3-D slices that intersect at a pixel of interest (POI): one slice displays range vs. azimuth (top view), another slice displays elevation vs. azimuth (front view), and the last slice displays elevation vs. range (side view). Along the azimuth axis, values are displayed in the reverse to emulate the SAR path taken by the vehicle during data collection. Along the elevation axis, the value of 0.0m is at ground/floor level. Values below ground/floor level appearing in the image represent the bottom part of the "curvature" created as a result of the point spread function. Viewing 2-D slices at different POIs provides a mechanism to manually detect the locations of targets of interest. When the POI is on-target at the highest intensity value of that target, the POI at that value becomes the pixel at maximum intensity (PMI). By convention, the radar path is always at the bottom for the top view images (truck going from right to left). Front view images are displayed as seen from the radar (truck going from right to left). Side view images are displayed with the radar to the left. The data were normalized to ensure scaling remained the same for all images. The image scaling factor of the relative power (dB) was set to [-90 0].

2.2 Human standing signature in free space

All targets were manually detected and the corresponding PMIs were identified. The signature of a human target in free-space is examined for different body positions. The positions include a human standing with arms at his side, a human standing with both arms stretched parallel to the ground, a human kneeling, a human holding an AK47 in a vertical position, a human holding an AK47 in an angled position, an empty chair, and a human sitting in a chair.

According to simulation studies of the signatures of the human body in free space conducted by the United States Army Research Laboratory [16], the main contribution to the radar return comes from the human torso. They conclude that arms and shoulders contribute to bright spots on the sides of the torso, that the legs contribute to a "late-time" return caused by the effect of double bouncing of the incident wave from one leg to the other before transmission to the receive antenna, and that there is significant backscatter appearing to come from behind the main return corresponding to the torso. A comparison of the results of those simulations using 3-D SAR images of human targets in free space was conducted in [17] for a human in the standing and arms stretched positions, with the added advantage of examining how the backscatter varies with elevation.

In this report, twelve different subjects were examined for the human standing position, standing between 8m and 12m away from the radar in range and standing on gravel or asphalt, as opposed to grass as was the case in [17]. Subjects varied in height and size. Resolution is less than 15cm in range and azimuth and 5.2 degrees in elevation. The strongest return can be seen at PMI elevations between the feet and the hips (less than 1m), which is different than the expected strongest return reported in [16] and what was observed in [17]. Given the elevation resolution of 1m at a distance of 10m from the radar, this suggests that the strongest return does not come from

the human torso but rather from the interaction between the ground and legs, where a corner is formed.

A typical 3-D SAR image is displayed as progressive top view 2-D slices at varying elevation in Figure 3 for elevations between -0.25m and 1.25m, at steps of 50cm (half the elevation resolution at a distance of 10m from the radar). The black lines show the locations of the slices which intersect at the PMI, with the value of 0.0m in elevation signifying at ground level. The strongest returns (0dB) occur at elevations from 0.25m to 1.25m. This 1m variation in elevation could be expected considering the elevation resolution. Two secondary returns (approximately -10dB) are present. They can be attributed to point scatterers located where the shoulder features are expected and where the double bounce from the leg features are expected, as was reported in the simulations of the human signature in [16]. The front and side view 2-D slices at the PMI of the 3-D SAR data in Figure 4 makes is possible to view the difference in elevation between the different features. In the front view image, the interaction between the ground and each foot is evident with a slight separation in azimuth between each feature. The strongest return is seen at knee level but a very strong return is also visible at the height corresponding to the human torso. In the side view image, the difference in range between the ground and leg interaction and the late return caused by the double bounce of the legs is discernible.

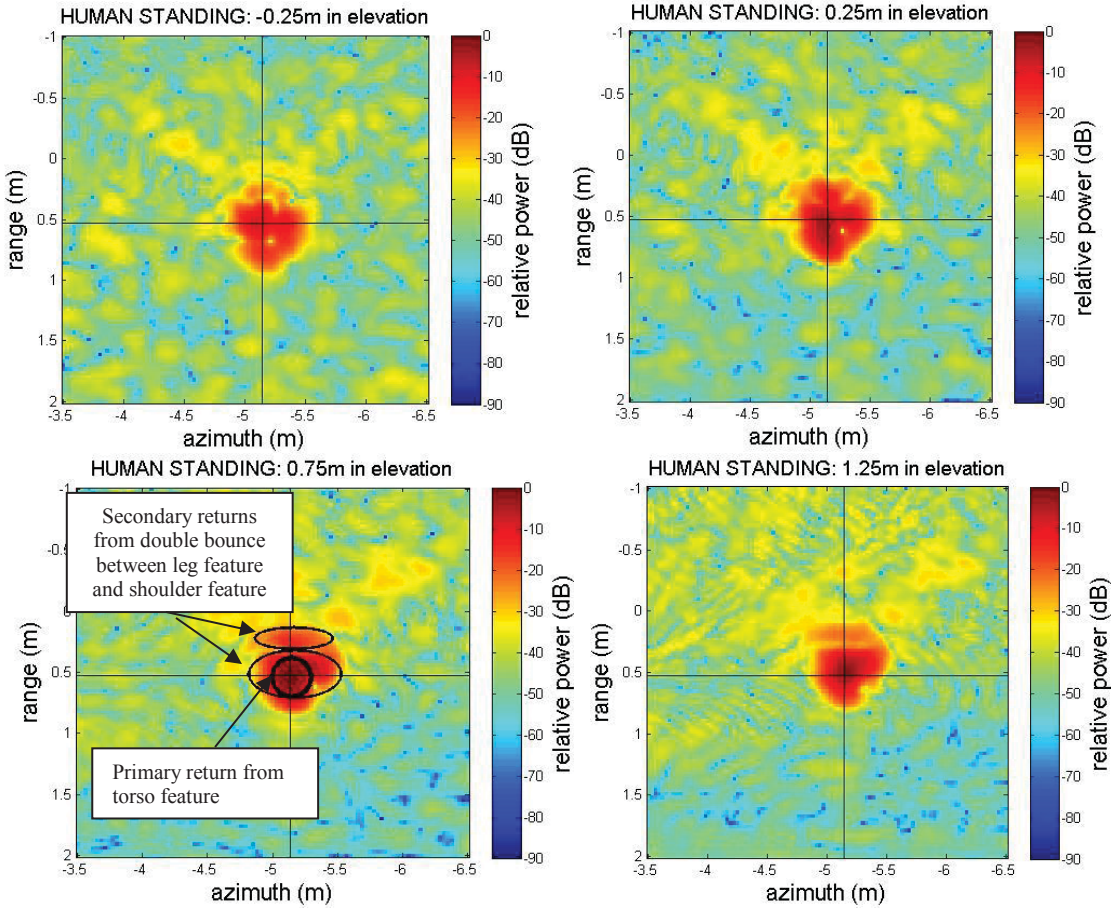

***Figure 3**: Top view 2-D slices of human target in standing position at varying elevations.*

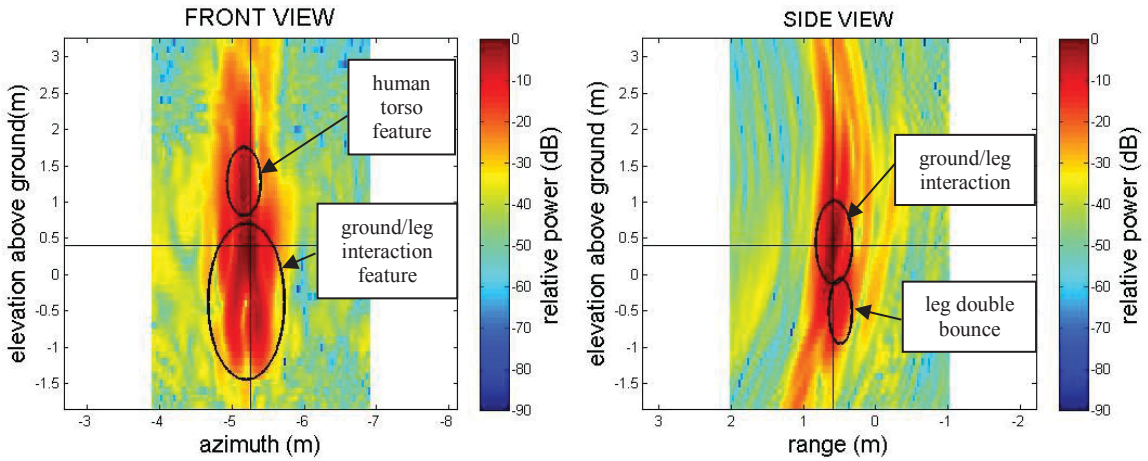

***Figure 4**: Front view and side view 2-D slices of human target in standing position.*

Variability in the human standing target signature was investigated to ensure the signatures were similar regardless of body shape and composition. Fifteen exemplars were observed for the twelve human subjects, some of which were targets more than once. They are labeled as H1 through H16. The top, front, and side view 2-D slices at the PMI of the 3-D SAR data of the human standing target for all exemplars is presented in 0. Five different signature characteristics were evaluated for each exemplar. They are listed below:

- Characteristic 1: PMI elevation coordinate at ground/leg interaction feature.
- Characteristic 2: shoulder feature present at PMI in top and side view.
- Characteristic 3: double bounce feature present at PMI in top view.
- Characteristic 4: slight separation in leg/ground interaction feature in front view.
- Characteristic 5: strongest return at center of signature in top view.

A table summarizing the results is shown in Table 1. Each characteristic is evaluated for each human standing target signature in free space. If the characteristic is present, the square is colored green. If the characteristic is not present, the square is colored red.

For most of the target signatures, the PMI elevation coordinate is at the height of the ground/leg interaction feature; whereas only three exemplars show a PMI elevation coordinate at the height of the torso feature (H4, H5, and H9). Of the fifteen target signatures, there are two target signatures where the shoulder feature does not appear in the image (H1 and H6). The double bounce feature is discernible in all cases. The slight separation of the ground/leg interaction feature is visible in all but one case (the third H1 exemplar). The strongest return is typically a blob at the center of the signature. In the cases where the PMI elevation coordinate is closer to the ground and the slight separation of the ground/leg interaction feature is present, there can be two strong return blobs about 50cm apart (H3, H8, and H9) or where one is more or less stronger than the other (H4, H5, H7, and H11).

***Table 1**: Variability in human standing target signature.*

	Characteristics 1	Characteristics 2	Characteristics 3	Characteristics 4	Characteristics 5
H1					
H1					
H1					
H2					
H3					
H4					
H4					
H5					
H6					
H7					
H8					
H9					
H10					
H11					
H12					

The analysis shows that there is some variability in the data but all have at least three of the five discernible characteristics. Photographs of each human standing target show some variability in how a human stands. For instance, some stand with feet wider apart than others. Some of the variability seen could be accounted for this difference in stance. Other difference could be accounted for the difference in body size and composition as well as difference in attire (full army fatigues vs. regular civilian clothing). Variability is further investigated using metrics, as will be shown in Section 4.

2.3 Human signature in different positions

The top, front, and side view 2-D slices at the PMI of the 3-D SAR data of the human target in four different positions is shown in Figure 5. Positions include: standing with arms stretched, kneeling, holding AK47 at an angle, holding AK47 vertically. The top, front, and side view 2-D slices at the PMI of the 3-D SAR data of an empty chair and a human sitting in a chair are shown in Figure 6.

In the human standing with arms stretched images, the torso and the extended arms of the human are readily discernible in the top view. The extent of the arm features in azimuth is evident. The strong returns are caused by the corner created between the arms and the body. Significant returns are once again seen behind the main torso and at the ground level where the ground and legs form a corner.

In the human kneeling top view image, the forward knee feature appears closer in range on the left side while the back foot feature appears further in range and weaker on the right side. The difference in signature between the human standing and human kneeling is most evident in the front view image, where the energy is more concentrated near the ground level, giving the

appearance of a bulb. Furthermore, the ground/foot separation feature seen in the human standing case is not present in the human kneeling signature.

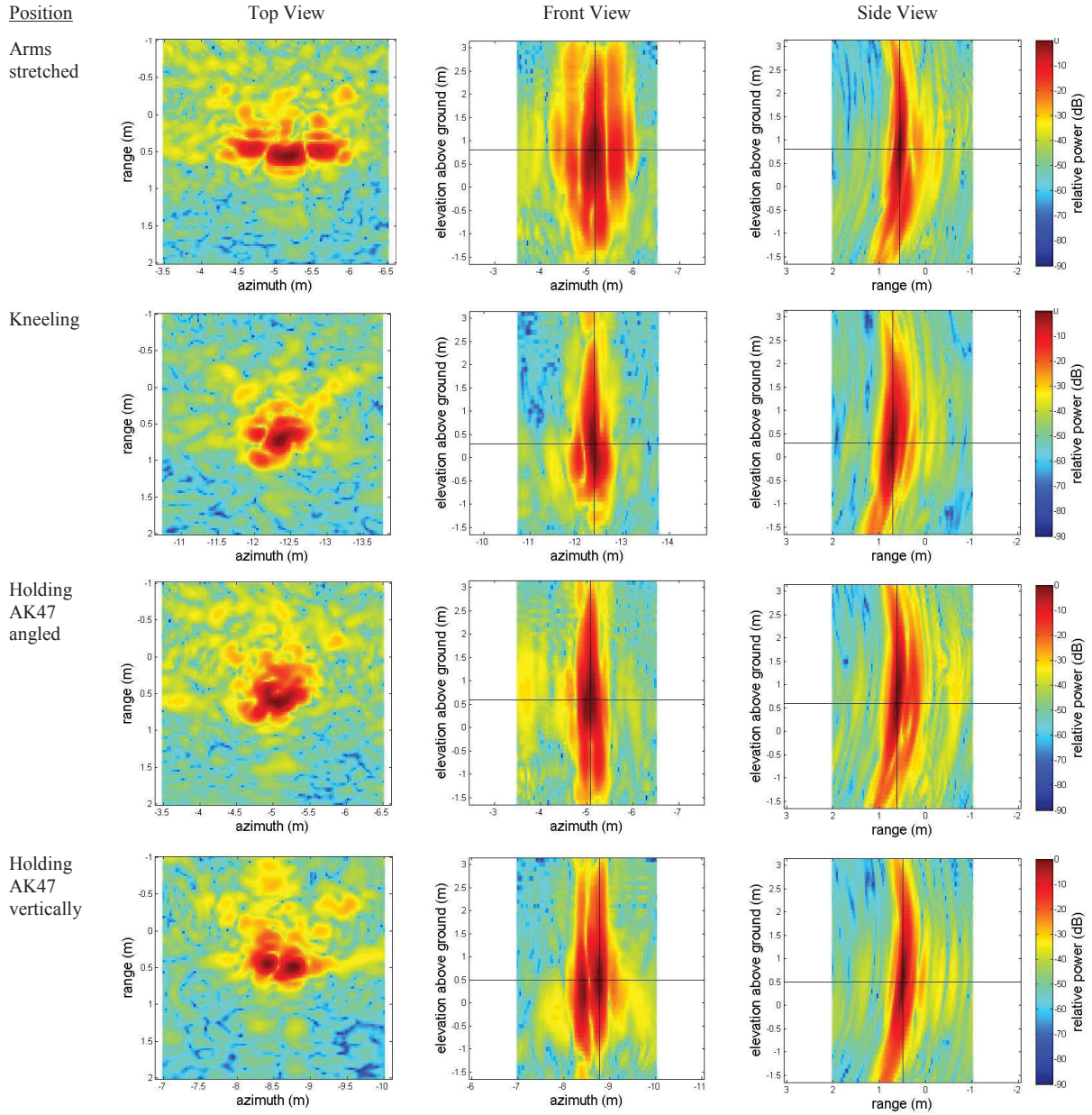

***Figure 5**: Top, front, and side view 2-D slices of human target in different positions.*

In the top view image of the human holding an AK47 in an angled position across its chest, the signature is very similar to the human kneeling one. The only discernible difference is the shape of the strongest return; more circular in the human kneeling case versus more of an arc in the human holding an AK47 in an angled position case. In the side view image, a late return that is brighter and extends further in range than the human standing case is visible. This is due to the multiple bounces between the AK47 and the human body, where many corners are formed.

In the human holding an AK47 vertically top and front view images, two distinct strong returns are visible side by side. One represents the human standing return while the other represents the AK47 return. Both are of the same intensity.

The signature of a chair in free space is presented in Figure 6. An analysis of the empty chair signature is presented in [17]. In the front view of the empty chair image, the two front chair leg returns are visible. In the side view of the image, the strongest return of the front legs is visible. The back legs and late return from the metallic bracket are visible further in range.

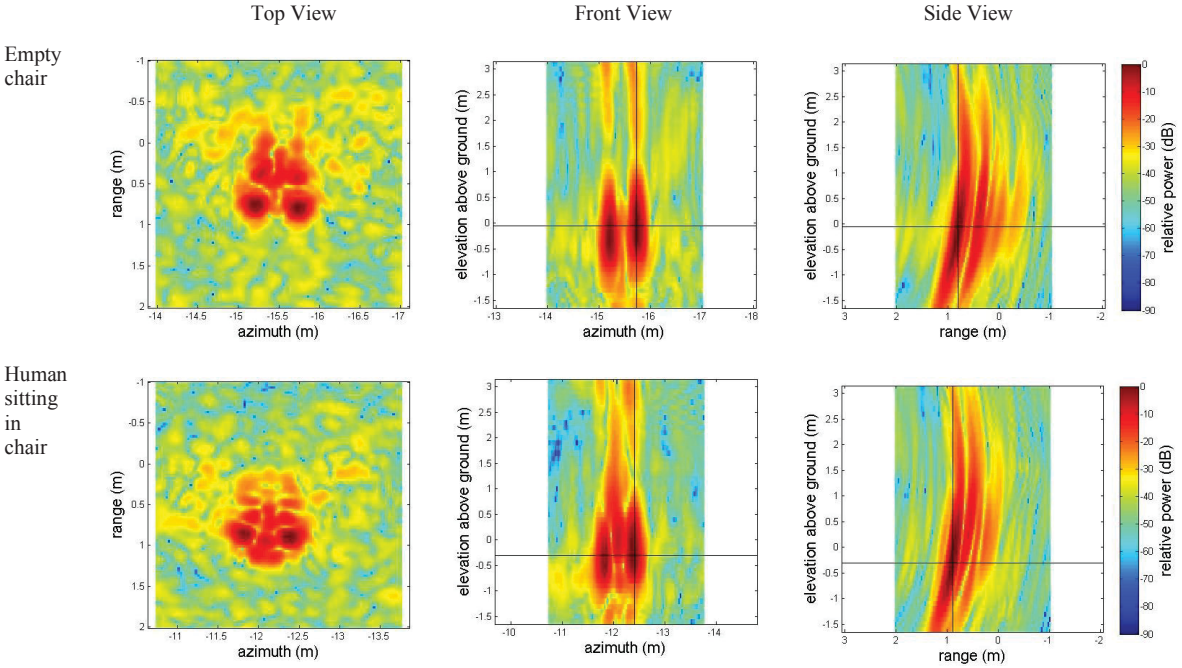

***Figure 6**: Top, front, and side view 2-D slices of empty chair and a human target sitting in chair.*

In the top view image of the human sitting in a chair, a strong return where the ground and the human legs create a corner is visible with the front chair leg features being brightest. Compared to the empty chair signature, the features of the back legs and the metallic brackets are weaker. This is due to the reduction in illumination from the radar signal as the signal now has to pass through and around the human to reach the back legs and brackets of the chair. The weaker returns further in range are also seen in the side view image. In the front view image, the strong return from the human is evident in between the two front chair leg returns.

In free space, the human standing signature can visually be differentiated from the human in different positions when looking at 2-D slices in the top, side, and front views. Having gained a better appreciation of the signatures of human targets in free space, the next step is to investigate what happens to the signature when the human is placed behind different wall materials.

3 Human target signatures behind walls

The signature of the human target in different positions behind three different wall structures is examined in this section. All targets were manually detected and the corresponding PMIs were identified. In Section 3.1, the human target signature behind drywall is analyzed. In Section 3.2, the human signature behind a cinder block wall is analyzed. In Section 3.3, the human target signature behind a brick/cinder block wall is analyzed.

3.1 Human signature behind drywall

The first wall structure is a fairly transparent one constructed of drywall made of wood studs, gypsum, insulating material, and vinyl coating on the exterior. A wooden bench with metallic legs surrounds the interior walls of the building. A LIDAR image of the inside of the building with the location of the human target is shown in Figure 7. The human target is positioned 1.6m behind the wall in between two windows. For this scenario, the signature of a human target is examined for four different body positions. The positions include a human standing, a human kneeling, a human holding an AK47 in an angled position, and a human holding an AK47 in a vertical position. The top, front, and side view 2-D slices at the PMI of the 3-D SAR data of the human target in these four different positions is shown in Figure 8. The location of the target is indicated by a black circle in the top view images. In each case, part of the wall signature appears at a range of -6m. Even behind a relatively transparent wall such as drywall, there is a significant increase in the amount of clutter and multipath.

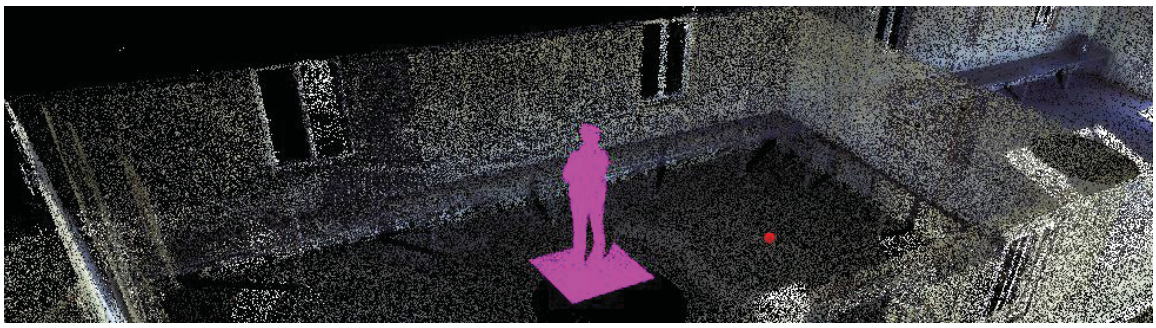

***Figure** 7: LIDAR imagery of a human standing inside a building constructed of drywall made of wood stud, gypsum, insulating material, and vinyl coating.*

In the human standing images, three bright spots at the location of the target at the same range are visible in the top view where only one bright spot is expected. They are all circular in shape. The middle return is similar to the one seen in free space but appears out of focus. This is expected considering the different paths through the wall structure that the radar signal must travel to get to the target, such as through and around studs. The different features from the floor/leg interaction, shoulders, and double bounce from the leg that were visible in the free space case are not discernible. In the front view image, the strong return from the floor/leg interaction combined with the strong return from the torso seems to dominate the signature. A small separation between the ground and each foot that was seen with the human standing in free space signature is also visible here. In the side view image, it is difficult to differentiate the late return from the double

bounce of the legs and the clutter. The two bright spots on each side of the main human signature could be ghosts, caused by multipath. This phenomenon is currently being investigated.

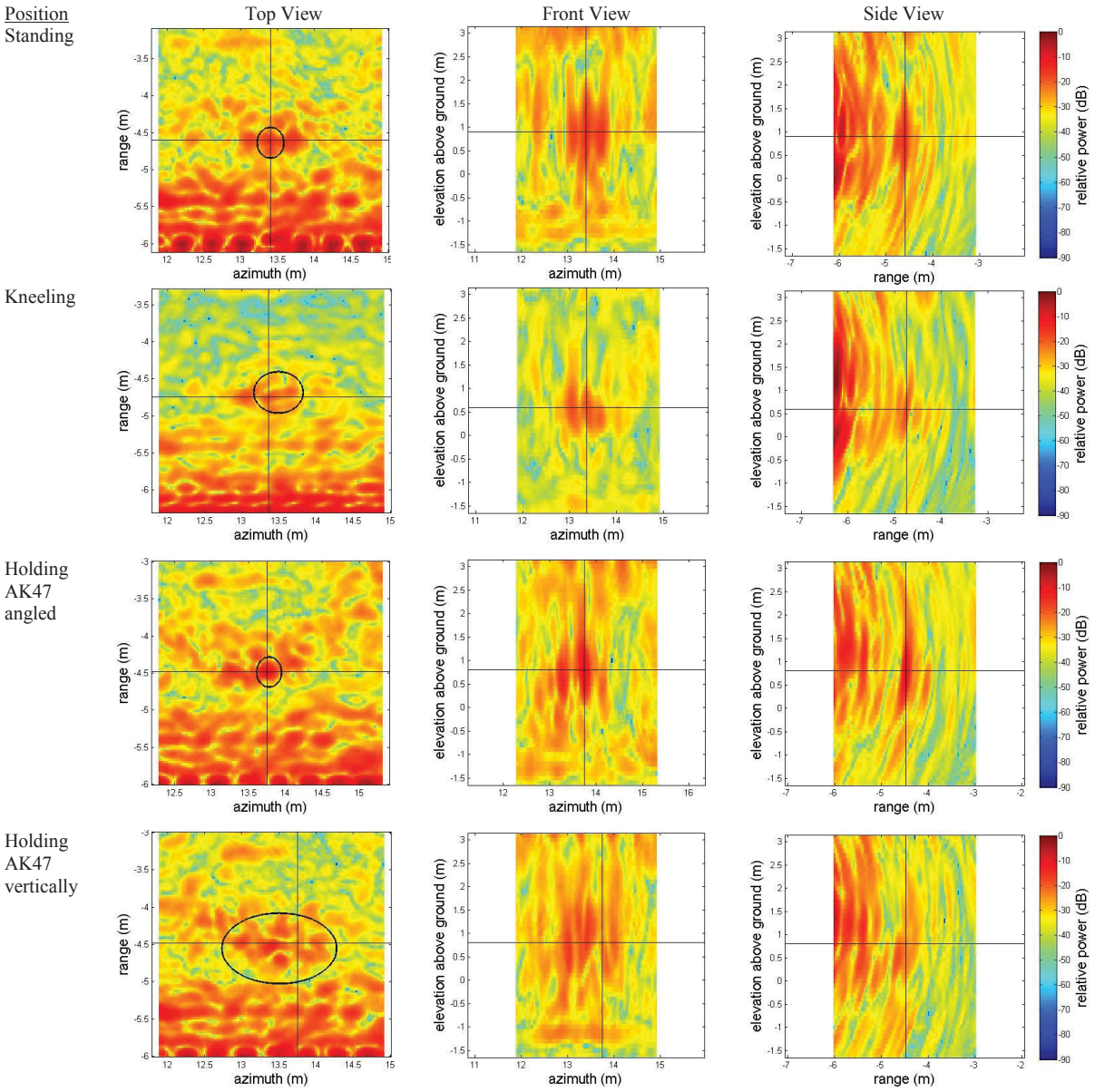

***Figure 8**: Top, front, and side view 2-D slices of human target in different positions behind a wall constructed of drywall made of wood stud, gypsum, insulating material, and vinyl coating.*

In the human kneeling top view image, two similarly strong returns are visible diagonally from each other. The right strong return is the target signature whereas the left strong return could be a ghost. The forward knee and back foot features of both returns are still visible, similarly to the free space human kneeling signature. In the front view image, there is considerably less energy in higher elevation for the kneeling target compared to the human standing behind the wall case.

For the return that could be a ghost, the energy is spread higher in elevation. In the side view image, it is difficult to differentiate the strong returns from the clutter.

In the stop view image of the human holding an AK47 in an angled position across its chest, the signature is very different from the human kneeling one. It resembles more of the human standing signature behind the wall. Three bright spots are visible at slightly different ranges. In the front view image, the two side returns are visible at the same elevation. In the side view image, the late return due to the multiple bounces between the AK47 and the human body is present. In the human holding an AK47 vertically top view image, there are several strong returns visible. It is difficult to distinguish between the different features. Several ghosts could be overlapping with the main returns, giving the appearance of a highly cluttered environment. Clutter also seems to overwhelm the front view image.

The biggest challenge of human detection in a fairly transparent wall structure like drywall is the amount of multipath and ghosts that are present. Discovering the cause of these phenomena and mitigating them could go a long way to helping increase detectability while lowering false alarms.

3.2 Human signature behind cinder block wall

The second wall structure is made of cinder blocks and is a more challenging wall to penetrate with the radar. A photograph of the inside of the building is shown in Figure 9. The human target is positioned 1.6m behind the wall for this scene. The wall structure being imaged contains no window or door. For this scenario, the signature of a human target is examined for six different body positions. The positions include a human standing with arms at his side, a human standing with both arms stretched parallel to the ground, a human kneeling, a human holding an AK47 in a vertical position, a human holding an AK47 in an angled position, an empty chair, and a human sitting in a chair. The top, front, and side view 2-D slices at the PMI of the 3-D SAR data of the human target in five different positions are shown in Figure 10. The top, front, and side view 2-D slices at the PMI of the 3-D SAR data of an empty chair and a human sitting in a chair are shown in Figure 11. In order to create greater contrast between the target and the background in the image, the image scaling factor of the relative power (dB) was changed from [-90 0] to [-40 0]. The location of the target is indicated by a black circle in the top view image. Part of the wall signature appears at a range of -0.5m.

***Figure 9**: LIDAR imagery of a human standing inside a building constructed of cinder blocks.*

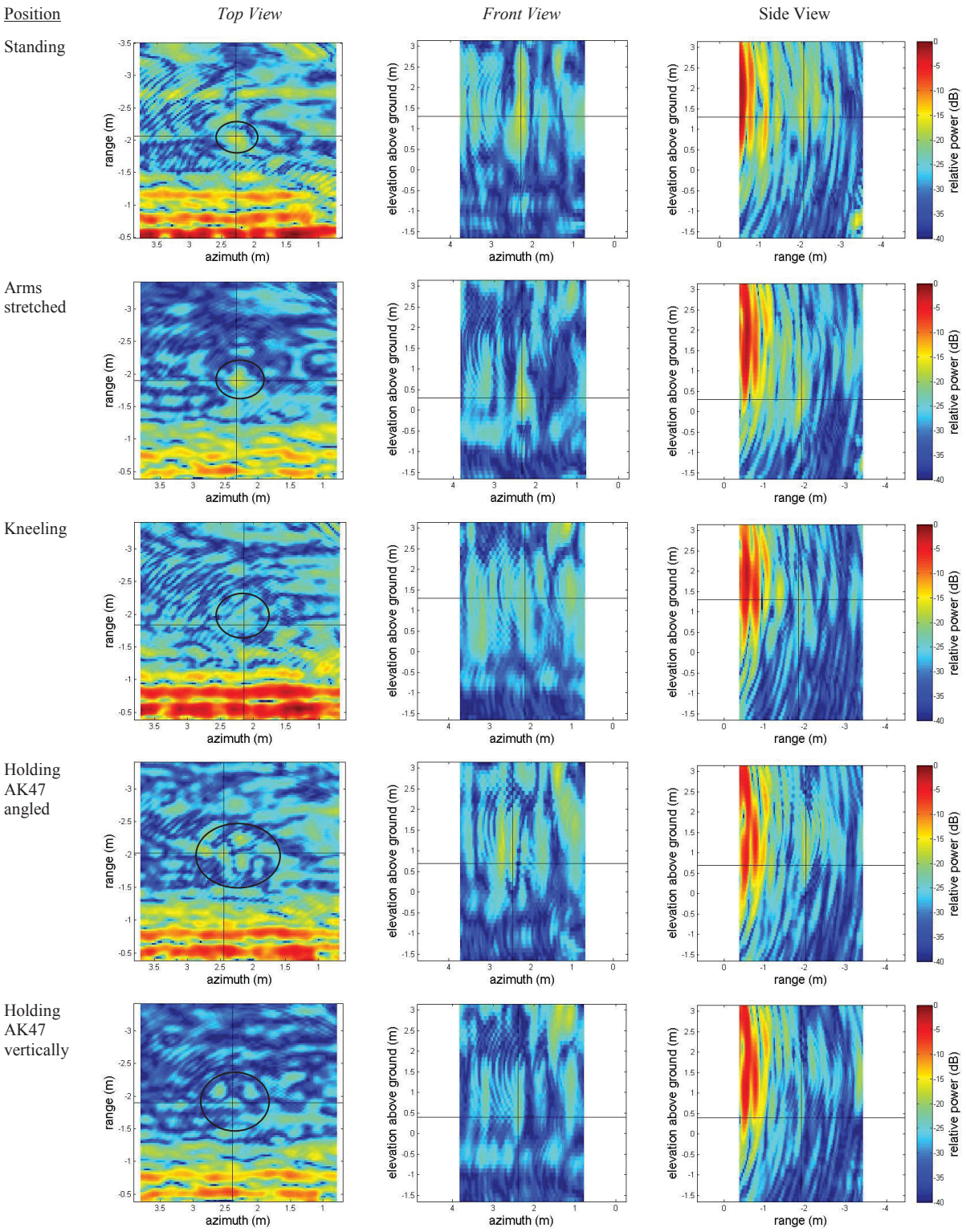

***Figure 10**: Top, front, and side view 2-D slices human target in different positions behind cinder block wall.*

In the human standing images, one bright spot at the location of the target is visible in the top view image. The strong return is oval and similar to the one seen behind a drywall structure but without the possible ghosts on each side. The strong return is not as discernible. This is expected considering the different paths through the air gaps of the cinder blocks that the radar signal must travel to get to the target. Again, the different features from the floor/leg interaction, shoulders, and double bounce from the leg that were visible in the free space case are not discernible. Several other bright spots are visible in the image, some of which could be considered clutter and some could be ghosts. In the front view image, the strong return from the floor/leg interaction combined with the strong return from the torso seems to dominate the signature. The small separation between the ground and each foot that was seen with the human standing in free space signature is not visible here. In the side view image, the clutter overwhelms the image, as is to be the case for all other positions.

In the human arms stretched top view image, the torso and the double bounce features are discernible. The extent of the arm features in azimuth is not evident in both the top view and front view images as it was in free space.

In the human kneeling top view image, three similarly strong returns are visible diagonally from each other. The center strong return is the target signature whereas the right and left strong returns could be ghosts. The forward knee and back foot features of both returns are still visible, similarly to the free space human kneeling signature. In the front view image, there is considerably less energy in higher elevation for the kneeling target compared to the human standing behind the cinder block wall case.

In the top view image of the human holding an AK47 in an angled position across its chest, the signature is very different from the human kneeling one. Several bright spots are visible at slightly different ranges. It is hard to differentiate the actual signature from what could be ghosts. In the front view image, the two side returns are visible at the same elevation though a large amount of clutter is present as well.

In the human holding an AK47 vertically top view image, there are three strong returns visible with two of the returns appearing further in range. These two returns could be ghosts. The return closest in range appears similar to the human standing signature though the size of the return is much smaller, which is unexpected. In the front view image, only one return is discernible at the PMI range coordinate; whereas there were two returns side by side in free space.

The signature of a chair in free space is presented in Figure 11. The amount of clutter is so prevalent that it is almost impossible to discern the chair features such as the two strong front leg returns as well as the two back leg returns and the bracket return. The same can be said for the signature of the human sitting in the chair.

The biggest challenge of manual human detection in a cinder block wall structure is the amount of clutter present. The problem of human detection is further complicated by the amount of multipath and ghosts also present. Though the human can be manually detected in some of the cases, a more quantitative analysis is required to eliminate a large amount of returns that are similar to the human target signature.

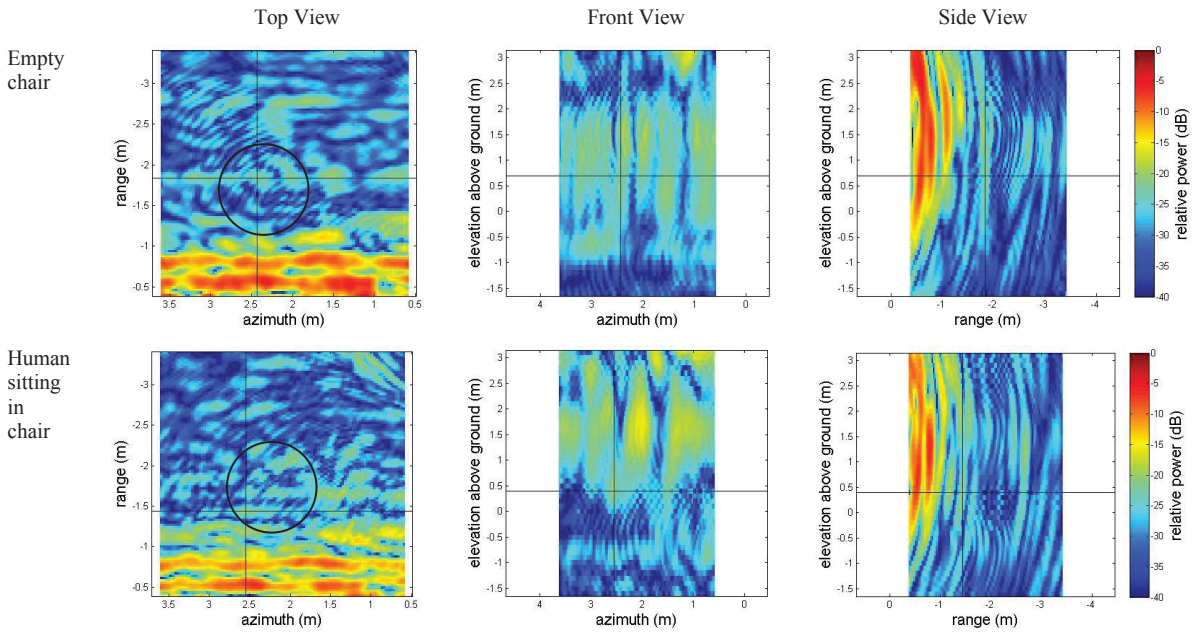

***Figure 11**: Top, front, and side view 2-D slices of empty chair and a human target sitting in chair behind brick/cinder block wall.*

3.3 Human signature behind brick/cinder block wall

The third wall structure is made of a layer of brick and a layer of cinder blocks. It is an even more challenging wall to penetrate with the radar than drywall or cinder block alone. A LIDAR image of the inside of the building with the location of the human target is shown in Figure 12. The human target is positioned 2.8m behind the wall. The wall structure contains no window. There is a large metallic garage door that was left open during data collection. With a beamwidth angle of 50 degrees, the human target is not illuminated by the radar system through the garage door. For this scenario, the signature of a human target is examined for three different body positions. The positions include a human standing with arms at his side, a human holding an AK47 in a vertical position, and a human holding an AK47 in an angled position. The top, front, and side view 2-D slices at the PMI of the 3-D SAR data of the human target these different positions is shown in Figure 13. The location of the target is indicated by a black circle in the top view image. Part of the wall signature is still visible at a range of -1.5m. In the images, the high clutter environment behind a brick/cinder block wall structure is evident. Even so, the human standing target can still easily be manually detected.

In the human standing images, one bright spot at the location of the target is visible in the top view image. The strong return is oval and similar to the one seen behind drywall and cinder block but appears more visible than the strong return seen behind cinder block. Again, the different features from the floor/leg interaction, shoulders, and double bounce from the leg that were visible in the free space case are not discernible. In this case, no other bright oval spots are visible in the image. In the front and side view images, the strong return from the floor/leg interaction combined with the strong return from the torso seems to dominate the signature.

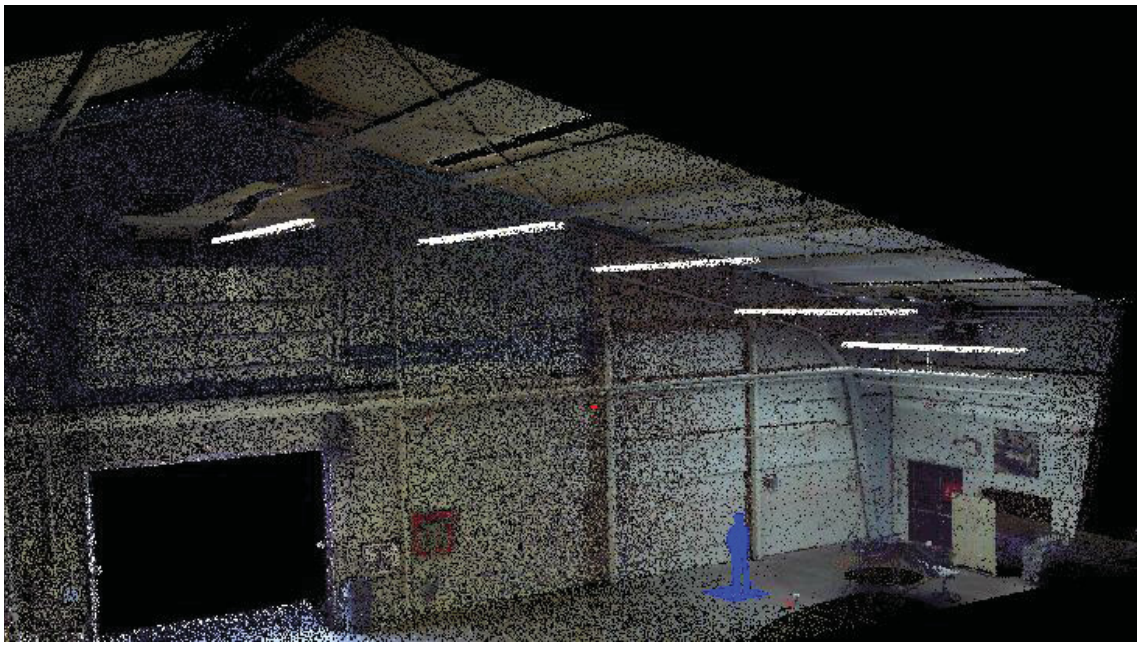

***Figure 12**: LIDAR imagery of a human standing inside a building constructed of brick/cinder blocks.*

In the top view image of the human holding an AK47 in an angled position across its chest, there is one strong return visible and no signs of what could be ghosts nearby. The signal is also slightly weaker than the human standing case, suggesting that a lot of the energy is not returned the radar. In the front and side view images, only one return is visible and weaker than the human standing case. The same can be said for the human holding an AK47 vertically top view image.

Manually detecting the human behind cinder block was challenging due to the low contrast between the target signature and the surrounding clutter/multipath blobs. It is surprising how the contrast is greater between the target signature and the surrounding clutter/multipath blobs in the case behind brick/cinder block considering the more challenging wall. It would be worthwhile to analyze another cinder block building from the 2012 Valcartier Trials to see if the same difficulties arise with cinder block alone or if that particular scene is noisier than normal.

Viewing of the SAR data as 2-D slices provides a qualitative means of discriminating between different target signatures. A more useful approach to discrimination would be to quantify these differences. In the next section, a look at different quantitative features as potential discriminants is investigated.

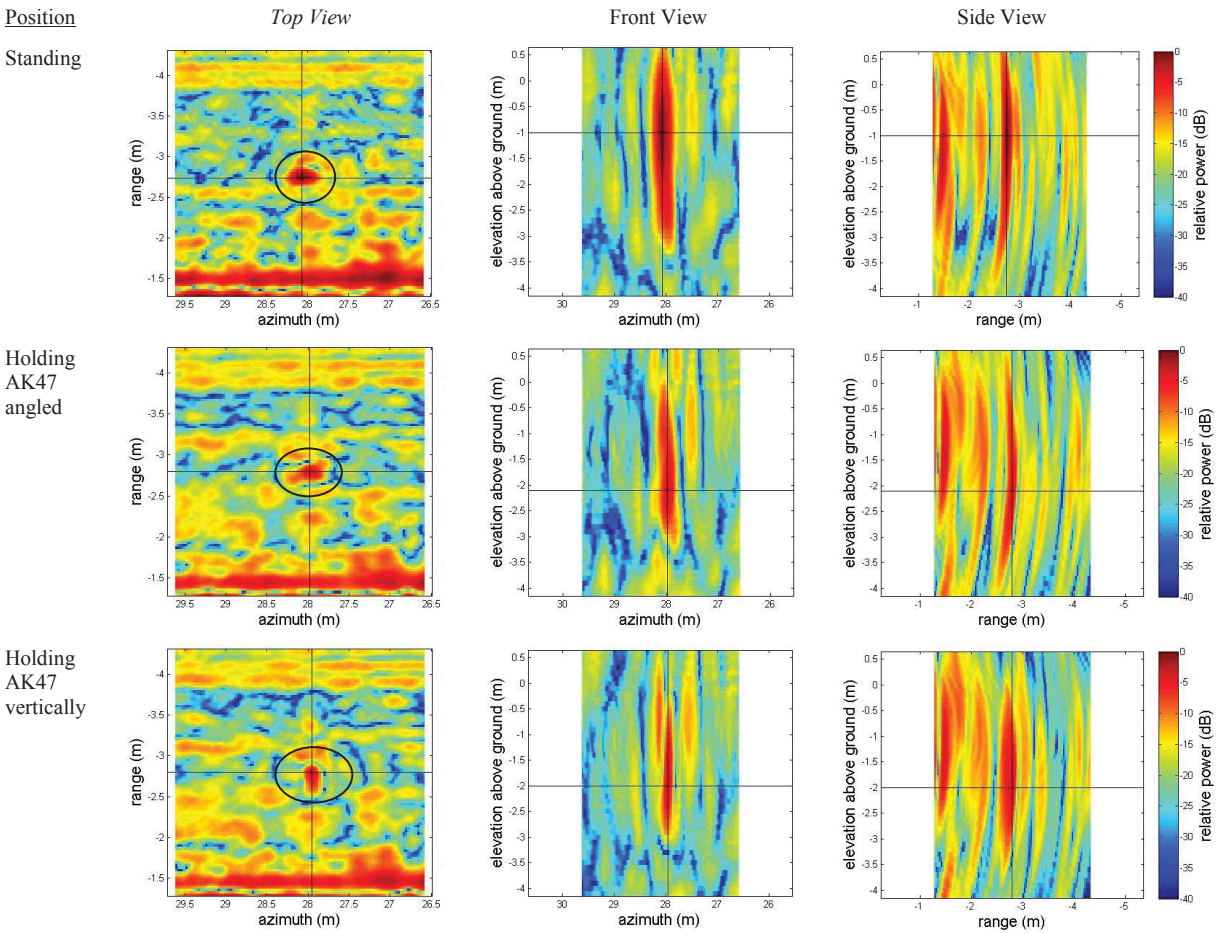

***Figure 13**: Top, front, and side view 2-D slices of empty chair and a human target sitting in chair behind brick/cinder block wall.*

4 Metrics for discrimination

The differences in human target signatures in different positions behind different wall structures were presented in Section 3. In this section, the potential quantitative features investigated in [17] for free space signatures are investigated here to determine viability for human target discrimination behind different wall structures. The six features investigated include the PMI elevation coordinate, the PMI intensity, the 3dB width in range and in azimuth, the maximum intensity profiles in range and in azimuth, the 3dB width profiles in range and in azimuth, and the number of resolution cells in range and azimuth for 3-D volumes.

Box plots were used to analyze the results. A box plot is a graphical representation of a distribution. The central red mark represents the median of the data. The edges of the blue box represent the 25^{th} and 75^{th} percentiles at the bottom and at the top, respectively. Whiskers extend maximally to 1.5 times the height of the central box but not past the range of the data. Outliers are plotted individually as red stars. The data in free space is separated in three categories. The first category (all data) includes all data regardless of their positions, the second category (standing) includes all data of the human in a standing position, and the third category (others) includes all data of the human in a position other than just standing [18].

Box plots of the PMI elevation coordinate data for each target in free space and behind walls were created and can be seen in Figure 14. In the free space case, sixteen exemplars of the human standing position and eight exemplars of the human in all other positions were used to form the box plots. In the case behind walls, four exemplars were used behind drywall, five exemplars were used behind cinder block, and three exemplars were used behind brick/cinder block, with the human target in various positions, with all data points indicated by a colored star.

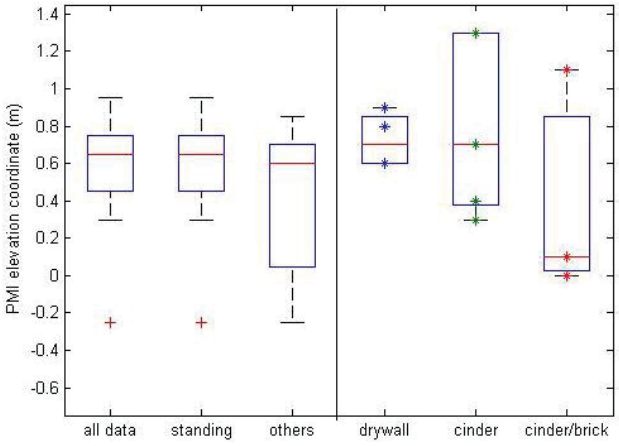

***Figure 14**: Box plots of PMI elevation coordinate for human (a) in free space and (b) human behind different wall structures.*

The PMI elevation of the human target standing in free space appears to be similar regardless of body position, though more variability exists with the human target in a position other than just standing. There is overlap between all box plots, in free space and behind walls. Though more exemplars behind walls are required to make definite conclusions, the PMI elevation metric should still be considered for human target discrimination behind walls.

Box plots of the PMI peak intensity value for each target in free space and behind walls were created and can be seen in Figure 15. The peak intensity is expected to be lower behind walls considering the attenuation that occurs as the radar signal penetrates the wall structure there and back. The attenuation through cinder block is expected to be lower than drywall and the attenuation through brick/cinder block is expected to be even lower than drywall and cinder block. The results in Figure 15 unexpectedly show a lower than expected attenuation through the brick/cinder block wall. There is the possibility there were issues with the cinder block wall data causing more clutter to be present in the imagery. This requires further investigation. It remains to be seen if this metric will be useful for human target discrimination behind walls.

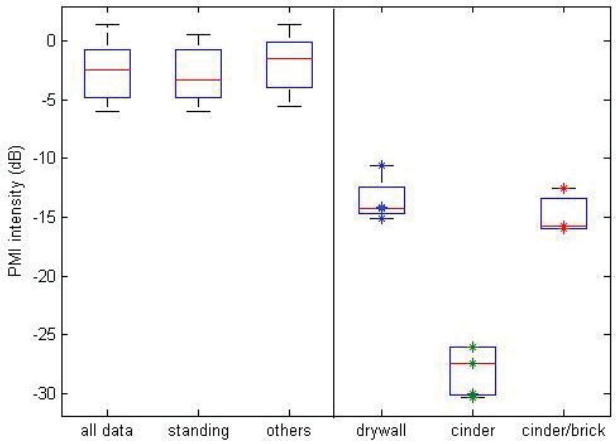

***Figure 15**: Box plots of PMI intensity for human in free space and human behind different wall structures.*

Box plots of the 3dB width in azimuth and in range for each target in free space and behind walls were created and can be seen in Figure 16. There is overlap between all box plots, in free space and behind walls. Though more exemplars behind walls are required to make definite conclusions, the 3dB width in azimuth and in range metrics should still be considered for human target discrimination behind walls.

The PMI was used as a seed point for a seed region growing algorithm to produce a 3-D volume as was done in [17]. A 10dB threshold was set to ensure that all human target signature features were present in the 3-D volume produced. Box plots of the number of resolution cells in azimuth and range for all 3-D volumes for each target in free space and behind walls were created and can be seen in Figure 17. In most cases, the number of resolution cells in azimuth and range for the human targets behind walls correspond closely to the number of resolution cells in azimuth and range for the human targets in free space. A clear distinction between the number of resolution cells in azimuth and range for 3-D volumes of the human targets behind cinder block is visible. In the cinder block case, the seed region growing algorithm might also be picking up ghosts or clutter/multipath. Though more exemplars behind walls are required to make definite conclusions, the number of resolution cells for 3-D volumes produced using a seed region growing algorithm in azimuth and in range metrics should still be considered for human target discrimination behind walls.

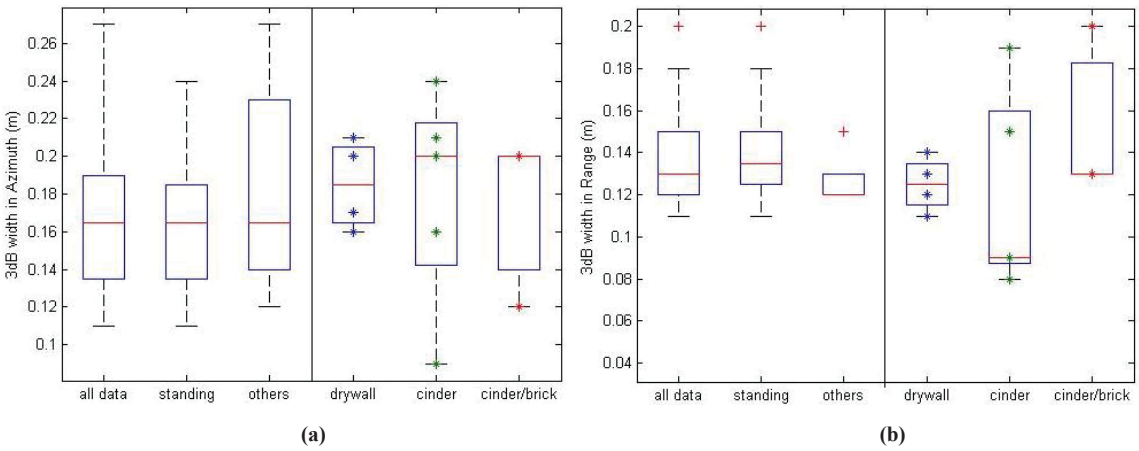

***Figure 16**: Box plots of 3dB width in (a) azimuth and (b) range for human in free space and human behind different wall structures.*

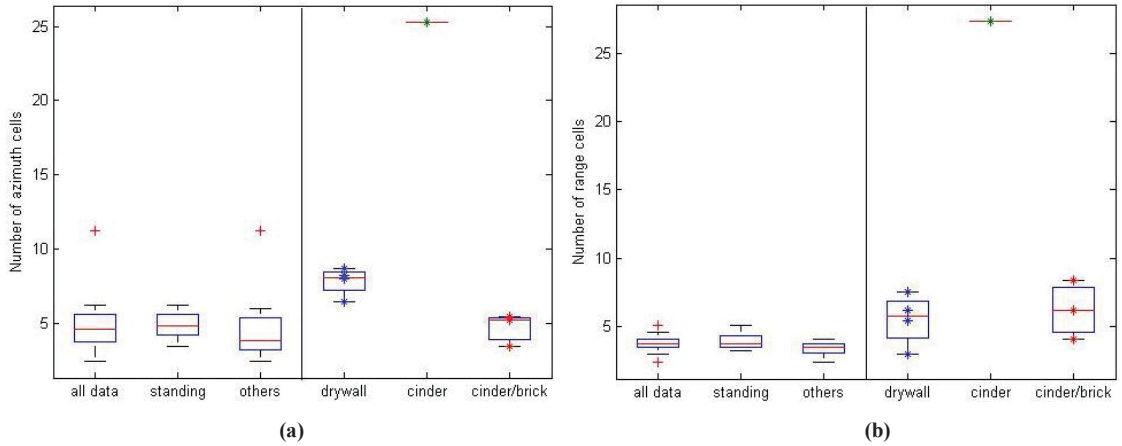

***Figure 17**: Box plots of number of (a) azimuth and (b) range cells for human in free space and human behind different wall structures.*

Variations in the maximum intensity in range in the azimuth direction for increasing distances from the PMI were investigated. Similarly, variations in the maximum intensity in azimuth in the range direction for increasing distances from the PMI were also examined. These two dimensions were chosen due to their higher spatial resolution. The creation of the profile of maximum intensities is described in [20]. The range and azimuth maximum intensity at varying range and azimuth locations, respectively, were determined for all targets. To quantify the difference between the range maximum intensity variations in the azimuth direction, a correlation matrix was obtained for all pairs of the profile curves. A color visual representation is given in Figure 18, where all humans in free space are marked as FS, humans behind drywall are marked as DW, humans behind cinder block are marked as CB, and humans behind cinder block/brick are marked as CBB. For this feature to be a good candidate for discrimination of the human target from all others, a strong correlation of 0.85 and above is desired between each pair of the profiles for the human in each of the different scenarios, namely, in free space, behind drywall, behind cinder block, and behind cinder block/brick. For cases involving other targets or noise behind walls, low correlation is desired between each pair for the human and all others.

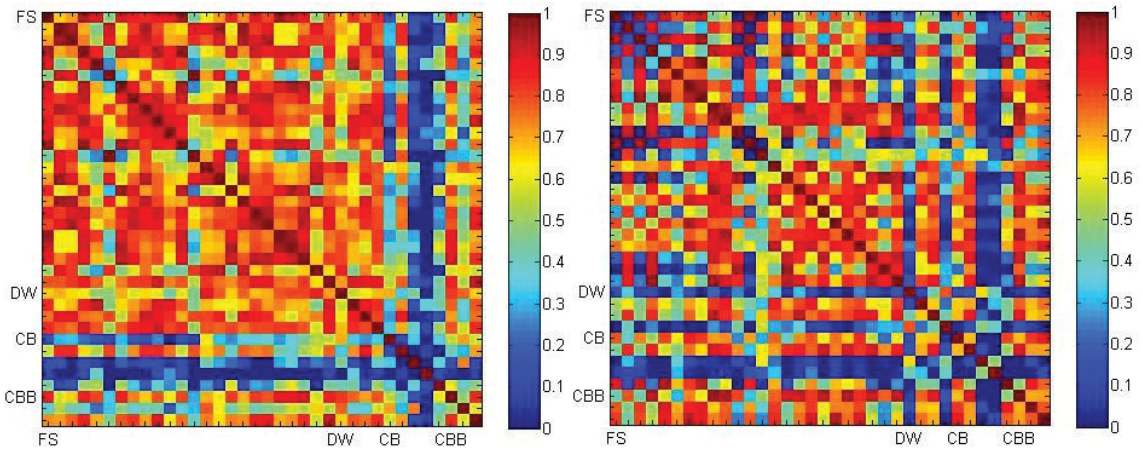

(a) **(b)**

***Figure 18**: Correlation matrix of maximum intensity in (a) azimuth at varying range positions for all targets and (b) range at varying azimuth positions for all targets.*

High correlation is observed in the correlation matrix of maximum intensity in azimuth at varying range positions between each pair of curves for the human targets in free space, behind drywall, and behind cinder block/brick; however, a low correlation exists between each pair of curves for the human targets behind cinder block. Though some high correlation is observed in the correlation matrix of maximum intensity in range at varying azimuth positions between each pair of curves, the variability between high and low correlation in each category is too high to make this a useful matrix.

The same evaluation was conducted for variations in the 3dB width in range in the azimuth direction for increasing distances from the PMI and similarly, variations in the 3dB width in azimuth in the range direction for increasing distances from the PMI were also examined. A color visual representation of the correlation matrix is given in Figure 19, where all humans in free space are marked as FS, humans behind drywall are marked as DW, humans behind cinder block are marked as CB, and humans behind cinder block/brick are marked as CBB. For this feature to be a good candidate for discrimination of the human target from all others, a strong correlation of 0.85 and above is desired between each pair of the profiles for the human in each of the different scenarios, namely, in free space, behind drywall, behind cinder block, and behind cinder block/brick. Low correlation is observed between almost all pairs of curves. This is clearly not a useful metric for human target discrimination behind walls.

The next step is to investigate the metric values for all suspected ghosts and clutter returns that are similar to the human target signature. The analysis can form the basis of finding discriminants to discriminate the human target from all others behind walls. It could prove useful in automating the process of human detection since current efforts are done manually by a SAR image analysis expert. This analysis is presented in the next section.

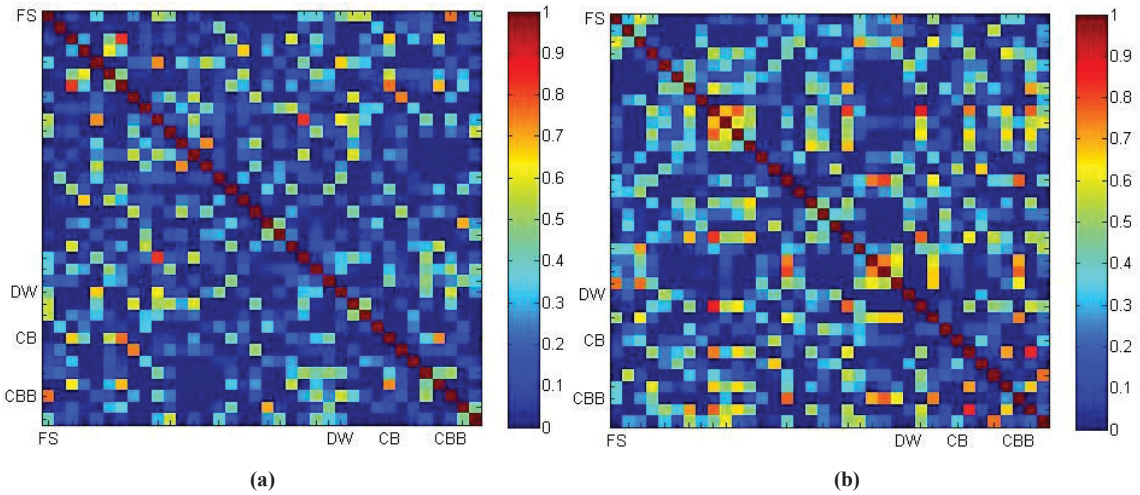

(a) **(b)**

***Figure 19**: Correlation matrix of 3dB width in (a) azimuth at varying range positions for all targets and (b) range at varying azimuth positions for all targets.*

5 Metrics applied to ghosts and clutter behind drywall

In this section, the potential quantitative features investigated in [17] and in Section 4 are investigated to determine viability for human target discrimination from ghosts, multipath, clutter, and wall signature behind a drywall structures. The six features investigated include the PMI elevation coordinate, the PMI intensity, the 3dB width in range and in azimuth, the maximum intensity profiles in range and in azimuth, the 3dB width profiles in range and in azimuth, and the number of resolution cells in range and azimuth for 3-D volumes.

The analysis is conducted on three scene containing five human targets inside a building constructed of drywall. The top view SAR image of one of the scenes is shown in Figure 20. The humans are placed approximately 1.5m and 1.8m from the wall and are not masked by the wall signature. On each side of the human target signature are what could possibly be ghosts. The wall signature including wall studs, windows, and other features are indicated in the image. Examples of clutter/multipath features used in the analysis are also indicated.

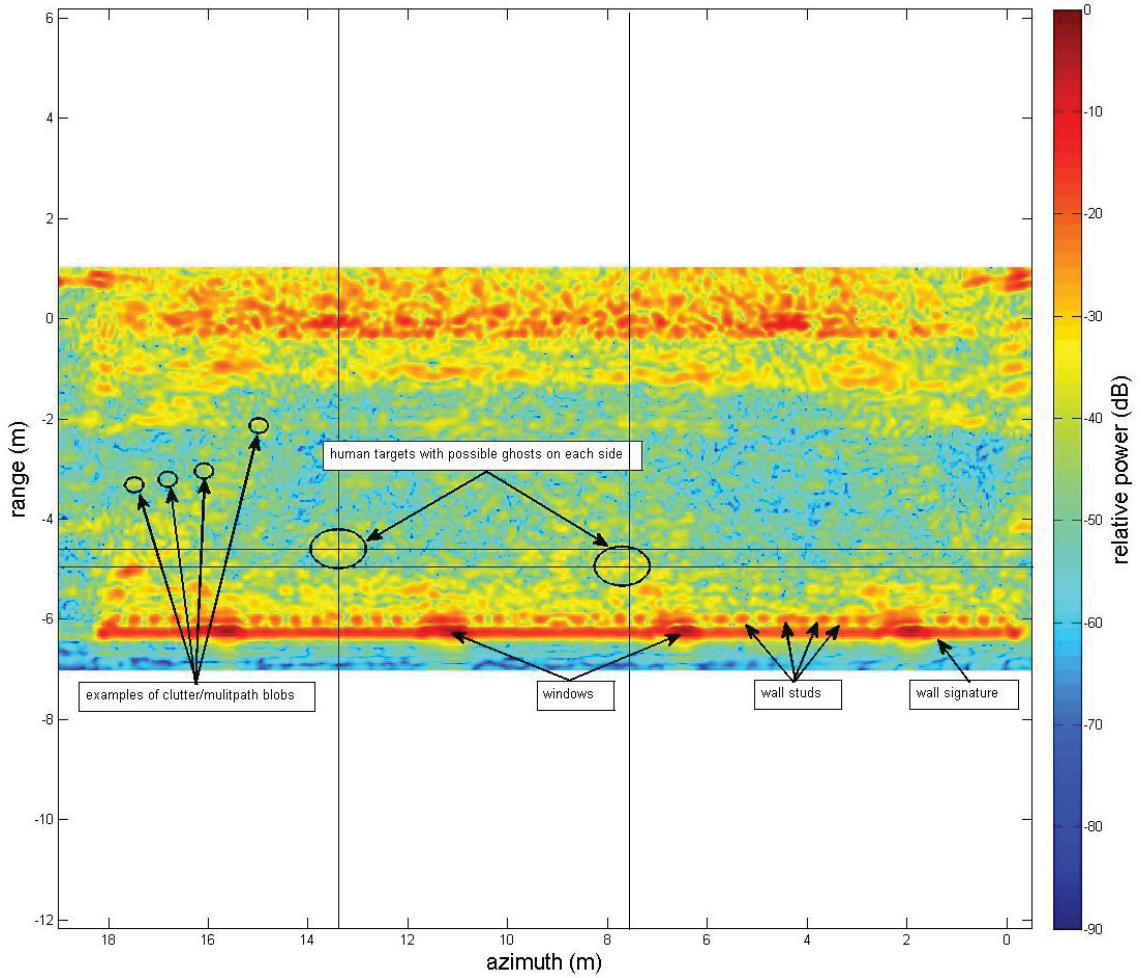

***Figure 20**: Top view SAR image of two human targets behind drywall.*

The PMI elevation coordinate data were extracted for both human targets, for the possible four ghosts, for twenty six exemplars taken from the studs of the wall signature, for twenty five exemplars taken from the wall signature features beyond the studs, and twelve exemplars taken from clutter at various locations in the scene. Box plots of the PMI elevation coordinate data for all exemplars were created and can be seen in Figure 21. Exemplars were divided into five different categories including human standing, possible ghosts, wall studs, other wall features, and clutter/multipath.

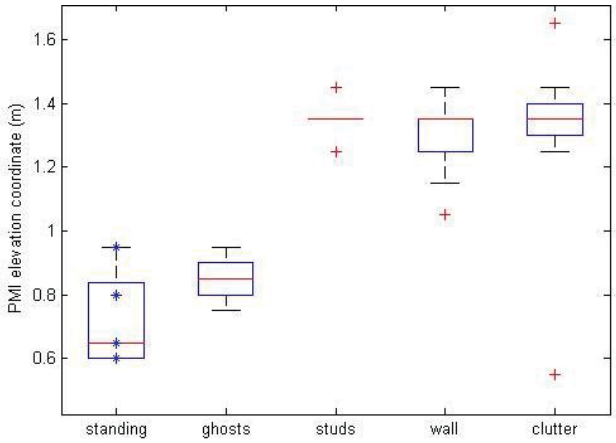

Figure 21*: Box plots of PMI elevation coordinate for different features of a scene containing two human targets behind a drywall structure.*

As seen in Figure 21, there is a discernible difference in PMI elevation coordinate values between the human target and the wall studs, other wall features, and clutter/multipath but little difference with the PMI elevation coordinate values between the human target and possible ghosts. The wall studs and other wall features can be completely discriminated from the human target as no overlap exists. Outliers from clutter/multipath contribute to overlap with the box plot of the human target, indicating that some false positives could arise with this metric. Despite this, the PMI elevation coordinate feature is a good candidate for discriminating the human target behind drywall although it cannot discriminate against possible ghosts in the image and could give rise to some false positives when considering clutter/multipath.

The PMI intensity data were extracted for all exemplars in the scene. Box plots of the PMI intensity for all exemplars were created and can be seen in Figure 22. There is a discernible difference in peak intensity values between the different exemplars although some overlap exists. The wall studs can be completely discriminated from the human target as no overlap exists. There is a slight overlap with between the human standing and the wall signature features and clutter/multipath box plots. The PMI intensity metric is a good candidate for discriminating the human target behind drywall; however, like the case with the PMI elevation coordinate metric, it cannot be used to discriminate fully. Other discriminants are needed to fully and robustly discriminate the human target from all other features in the scene.

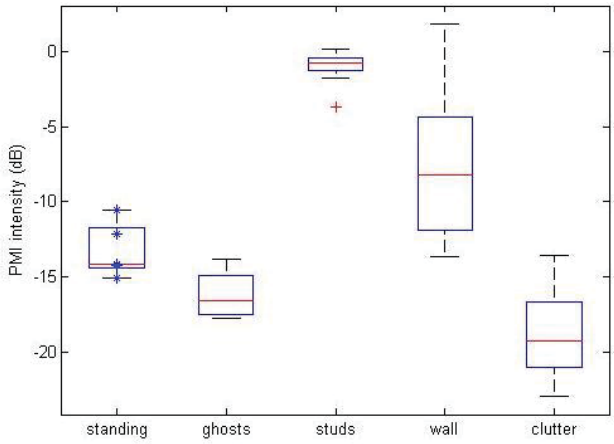

***Figure 22**: Box plots of PMI intensity for different features of a scene containing two human targets behind a drywall structure.*

Box plots of the 3dB width in azimuth and in range for all exemplars can be seen in Figure 23. Considerable overlap can be seen in almost every case. The possible ghosts are the only features that can be completely discriminated from the human target for the 3dB width in azimuth case as no overlap exists. Some overlap between the human target box plot and outliers of the studs feature box plot exists which could contribute to some false positive results. Considering this is the first metric that can discriminate the human target from the possible ghosts, the 3dB width in azimuth metric is a good candidate from discriminating the human target behind drywall. There is overlap with every box plot in the 3dB width in range case. The 3dB width in range metric is less appealing for human target discrimination behind a drywall structure.

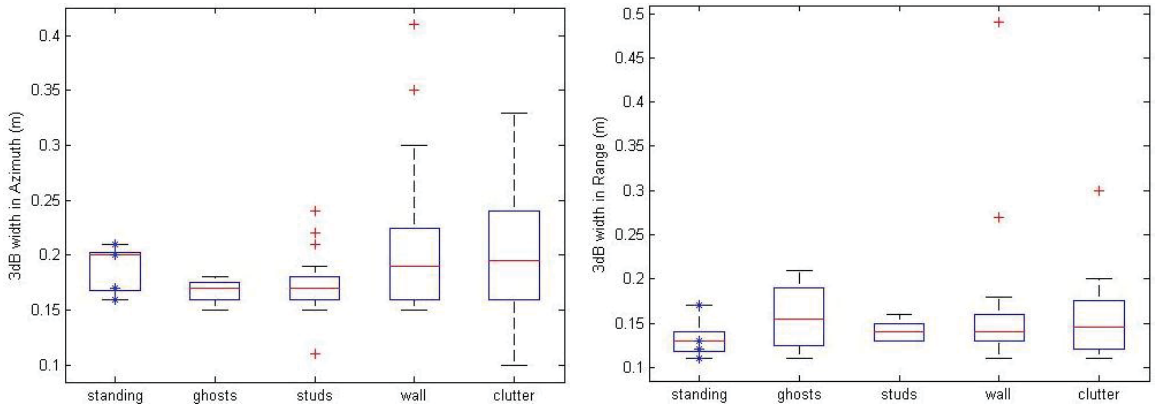

***Figure 23**: Box plots of 3dB width in (a) azimuth and (b) range for different features of a scene containing two human targets behind a drywall structure.*

The PMI was used as a seed point for a seed region growing algorithm to produce a 3-D volume as was done in [17]. A 10dB threshold was set to ensure that all human target signature features were present in the 3-D volume produced. Box plots of the number of resolution cells in azimuth and range for 3-D volumes for all exemplars can be seen in Figure 24.

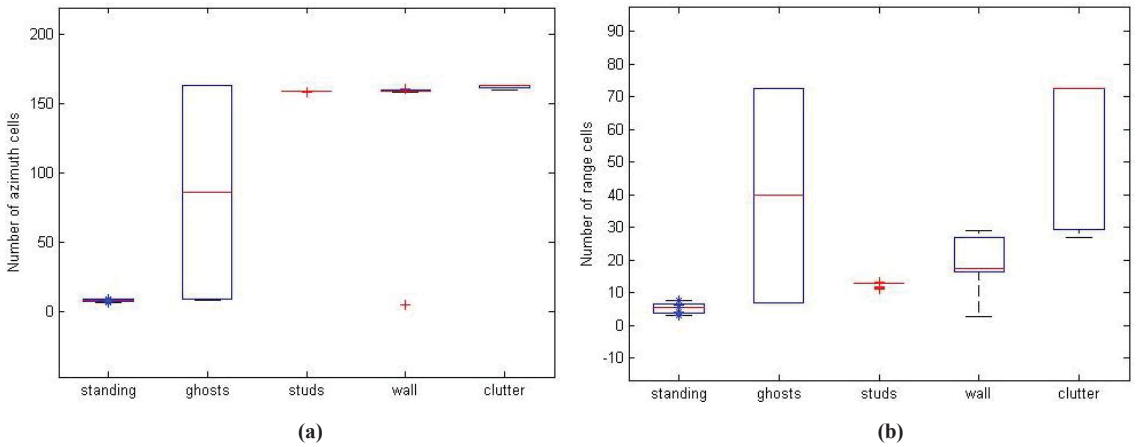

***Figure 24**: Box plots of number of (a) azimuth and (b) range cells for human in free space and human behind different wall structures.*

There is a discernible difference in the number of resolution cells in azimuth between the human target and all other features. The high number of azimuth and range cells seen is equivalent to the size of the building and can be attributed to the fact that the seed region growing algorithm picks up all the surrounding ghosts, studs, wall features, and clutter/multipath to form the 3-D blob when the PMI of these features other than the human target is used as the seed point. The wall studs and the clutter/multipath features can be completely discriminated from the human target as no overlap exists. Only one outlier from the other wall signature features and two values from the possible ghost features contribute to the overlap with the box plot of the human target, which gives rise to three false positive results in 69 exemplars.

Though there is still a discernible difference in the number of resolution cells in range between the human target and all other features, the difference is not as great as in the number of resolution cells in azimuth metric. The wall studs and the clutter/multipath features can also be completely discriminated from the human target as no overlap exists. As with the number of resolution cells in azimuth metric, two of the four values from the possible ghost features contribute to the overlap with the box plot of the human target. This time, there are three values from the other wall signature features that contribute to the overlap with the box plot of the human target.

The number of resolution cells in azimuth and range of 3-D volumes are excellent metrics to consider for human target discrimination behind a drywall structure.

Variations in the maximum intensity in range in the azimuth direction for increasing distances from the PMI were investigated for all exemplars. Similarly, variations in the maximum intensity in azimuth in the range direction for increasing distances from the PMI were also examined. A correlation matrix was obtained for all pairs of the profile curves, split into three images. The first image represents the correlation between human targets, possible ghosts, and wall studs. The second image represents the correlation between human targets, possible ghosts, and other wall signature features. The third image represents the correlation between human targets, possible ghosts, and clutter/multipath features. The color visual representations are given in Figure 25. For this feature to be a good candidate for discrimination of the human target from all others a strong

correlation of 0.85 and above is desired between each pair of the profiles for the human target and a weaker correlation of less than 0.6 is desired between each pair for the human and all others.

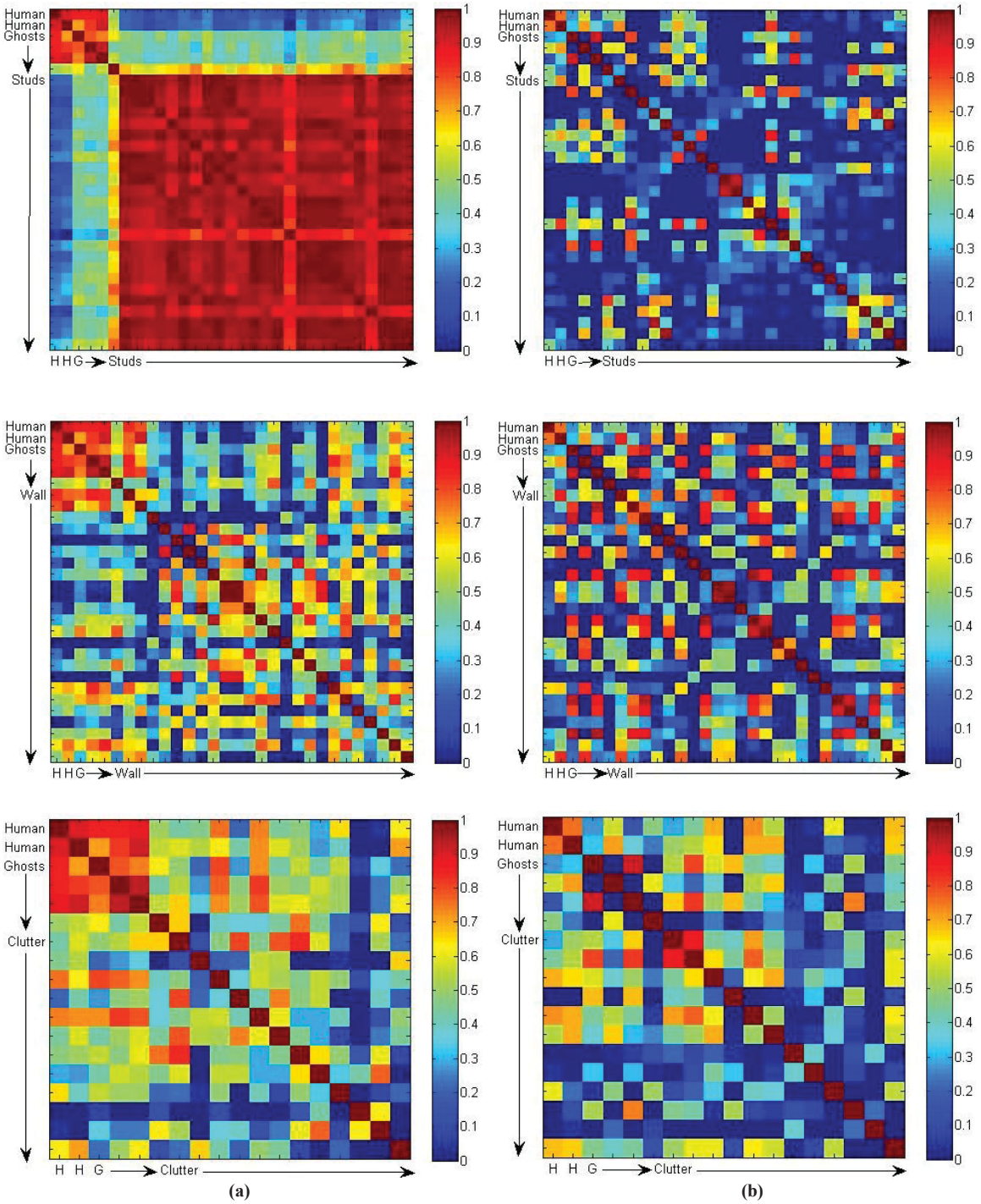

***Figure 25**: Correlation matrix of maximum intensity in (a) azimuth at varying range positions for all targets and (b) range at varying azimuth positions for all targets.*

As seen in the images of Figure 25(a), high correlation is observed between each pair of curves for the human target and for the human target and ghosts when considering the maximum intensity profiles in azimuth at varying range positions. High correlation is also observed between each pair of curves for the wall stud features. Low correlation is observed between each pair of curves between the human target and the wall stud features, the other wall signature features, and the clutter/multipath features. Complete discrimination between the human targets and the wall stud features is possible with the maximum intensity profile in azimuth at varying range positions metric. With this metric, a high level of discrimination between the human target and all others except for the possible ghost features is also possible though a small number of false positives are present. This metric is a good one to consider for human target discrimination behind a drywall structure. As seen in the images of Figure 25(b), low correlation is observed between most pairs of curves, including between human targets, when considering the maximum intensity profiles in range at varying azimuth positions. This metric is a poor one for human target discrimination behind a drywall structure.

Variations in the 3dB width in range in the azimuth direction for increasing distances from the PMI were investigated for all exemplars. Similarly, variations in the 3dB width in azimuth in the range direction for increasing distances from the PMI were also examined. A correlation matrix was obtained for all pairs of the profile curves, split into three images. The first image represents the correlation between human targets, possible ghosts, and wall studs. The second image represents the correlation between human targets, possible ghosts, and other wall signature features. The third image represents the correlation between human targets, possible ghosts, and clutter/multipath features. The color visual representations are given in Figure 26. For this feature to be a good candidate for discrimination of the human target from all others a strong correlation of 0.85 and above is desired between each pair of the profiles for the human target and a weaker correlation of less than 0.6 is desired between each pair for the human and all others.

In all cases, low correlation is observed between most pairs of curves when considering both the 3dB width profiles in azimuth at varying range positions and 3dB width profiles in range at varying azimuth positions, including between human targets. Both metrics are poor ones for human target discrimination behind a drywall structure.

Ten metrics were investigated for the purpose of discriminating the human target behind a drywall structure from all other features in a scene. They are listed below:

- Metric 1: PMI elevation coordinate.
- Metric 2: PMI intensity value.
- Metric 3: 3dB width in azimuth.
- Metric 4: 3dB width in range.
- Metric 5: Number of resolution cells of 3-D volumes in azimuth.
- Metric 6: Number of resolution cells of 3-D volumes in range.
- Metric 7: Correlation between maximum intensity profiles in azimuth.
- Metric 8: Correlation between maximum intensity profiles in range.
- Metric 9: Correlation between 3dB width profiles in azimuth.
- Metric 10: Correlation between 3dB width profiles in range.

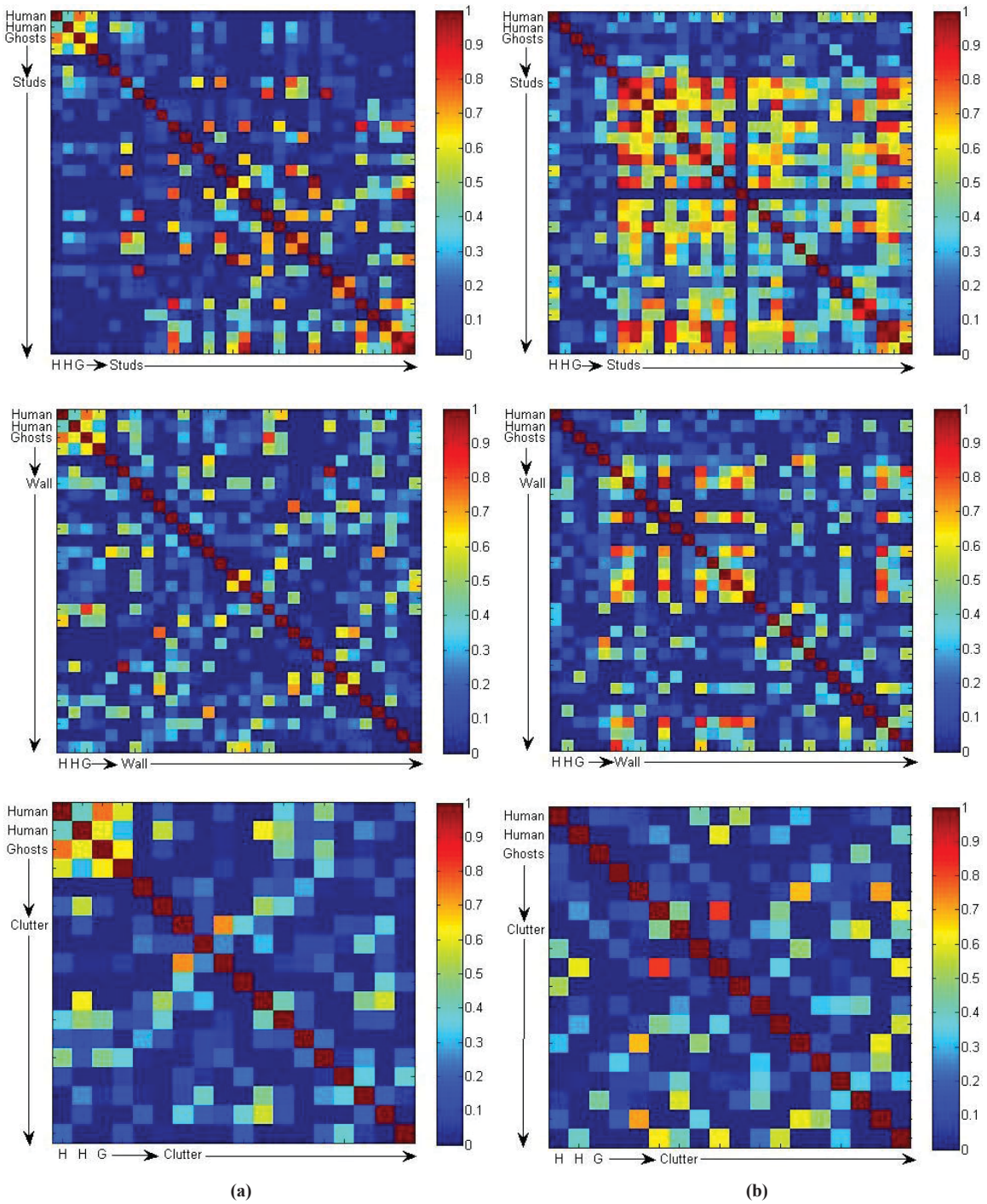

***Figure 26**: Correlation matrix of 3dB width in (a) azimuth at varying range positions for all targets and (b) range at varying azimuth positions for all targets.*

A table summarizing the results of the metric analysis is shown in Table 2 for all ten metrics. It indicates the metric's ability to discriminate the human target from the other features in a drywall scene. A green box indicates that the human target was fully discriminated; a yellow box indicates that the human target was discriminated in most cases; and a red box indicates that the human target was poorly discriminated. The analysis shows that not one single metric can fully discriminate the human target from all others but that a combination of a minimum of three metrics is required.

***Table 2**: Results from analysis for human target discrimination behind drywall.*

	Metric 1	Metric 2	Metric 3	Metric 4	Metric 5	Metric 6	Metric 7	Metric 8	Metric 9	Metric 10
Possible ghosts										
Wall studs										
Wall features										
Clutter/ multipath										

6 Discussion and conclusions

Tools and algorithms for 3-D visualization are being developed for the analysis of signatures of human targets behind a wall and to develop an understanding of the clutter and multipath signals in a room of interest. In this report, a comprehensive study of the characteristics of free-space and through-wall target signatures were presented using 3-D SAR data. The aim of this investigation was to gain a better appreciation of the signatures of targets placed behind different wall materials and to identify potential discriminants for classification of human targets. Radar signatures in 3-D SAR imagery were studied for the human target in different positions in free space and behind three different wall structures. There was very close agreement between simulations and the strong SAR image returns produced from the human standing target in free space. Most of the sources of the strong returns seen in the SAR images were explained, taking into consideration the location of the PMI, the measurements between different returns, and the location of the strong returns with respect to different physical features of each target, such as corners formed.

Variability between different human target signatures was investigated. Though differences exist, there is still enough commonality to have confidence in the metrics chosen for discrimination. The human target was manually detected in most cases behind the three different wall structures. The cinder block wall proved the most challenging for manual human target detection; however, metrics were similar to data in free space and behind the other wall structures. Further investigation as to why cinder block was more challenging to detect human targets than brick/cinder block is needed.

A comprehensive study of 3-D human target signature metrics in free space and behind three different wall structures was carried out. The six features investigated include the PMI elevation coordinate, the PMI intensity, the 3dB width in range and in azimuth, the maximum intensity profiles in range and in azimuth, the 3dB width profiles in range and in azimuth, and the number of resolution cells in range and azimuth for 3-D volumes. All features except the 3dB width profiles in range were still considered valuable metrics to consider for discrimination of the human target from all other targets.

A comprehensive study of metrics for 3-D human target signature and other features such as wall signature, possible ghosts, clutter and multipath behind a drywall building is also provided. The aim of this study is to identify features for discrimination of the human target from other similar features in an empty scene. Several metrics were investigated as potential discriminants and six specific ones were identified as good candidates. They include the PMI elevation coordinate, the PMI intensity value, the 3dB width in azimuth, the number of resolution cells of 3-D volumes in azimuth, the number of resolution cells of 3-D volumes in range, and the correlation between maximum intensity profiles in azimuth. Based on this study, no single metric could be used to fully discriminate the human targets from all others. A combination of at least three different metrics is required to achieve this.

Efforts will continue to investigate metrics for the purpose of human discrimination behind walls. A more thorough analysis of the drywall building scene will be conducted where all 3-D volumes will be tested against the six metrics considered valuable in this report. The analysis will encompass other drywall building scenes in order to evaluate detection and false alarm rates. Furthermore, metrics will be used to evaluate buildings of different construct such as cinder block

walls and cinder block/brick walls. Once the evaluation has been completed, the metrics will be implemented into an automatic human target detection algorithm for analysis.

This page intentionally left blank.

References

[1] Amin, M. G., [Through-the-wall RADAR imaging], CRC Press, Florida (2011).

[2] Prism 200: Through Wall Radar, Cambridge Consultants, June 11, 2014, http://www.cambridgeconsultants.com/projects/prism-200-through-wall-radar.

[3] Xaver Products, Camero, June 11, 2014, http://www.camero-tech.com/products.php.

[4] EMMDAR (Electro-Magnetic Motion Detection And Ranging), L3 CyTerra, June 11, 2014, http://www.cyterra.com/products/emmdar.htm.

[5] Range-R, L3 CyTerra, June 11, 2014, http://www.cyterra.com/products/ranger.htm.

[6] ASTIR : Standoff Through-Wall Imaging Radar, Akela, June 11, 2014, http://www.akelainc.com/products/astir.

[7] CPR-4, Cinside, June 11, 2014, http://cinside.se/e/produts/cinside-cpr4.

[8] O-PEN Radar, SRC, June 11, 2014, http://www.srcinc.com/what-we-do/radar-and-sensors/o-pen-radar.html.

[9] Ralston, T. S., Charvat, G. L., Peabody, J. E., "Real-time through-wall imaging using an ultrawideband multiple-input multiple-output (MIMO) phased array radar system," IEEE International Symposium on Phased Array Systems and Technology, 551-558 (2010).

[10] Chetty, K., Smith, G. E., Woodbridge, K., "Through-the-wall sensing of personnel using passive bistatic WiFi radar at standoff distances," IEEE Trans. On Geoscience and Remote Sensing, 50(4), 1218-1226 (2012).

[11] Riaz, M. M., Ghafoor, A., "Principle component analysis and fuzzy logic based through wall image enhancement," Progress in electromagnetic Research, 127, 461-478 (2012).

[12] Shirodkar, S., Barua, P., Anuradha, D., Kuloor, R., "Heart-beat detection and ranging through a wall using ultra wide band radar," IEEE International Conference on Communications and Signal Processing, 579-583 (2011).

[13] Sévigny, P., DiFilippo, D., Laneve, T., Chan, B., Fournier, J., Roy, S., Ricard, B., Maheux, J., "Concept of operation and preliminary experimental results of the DRDC through-wall SAR system, Proceedings of SPIE 7669, 766907, doi: 10.117/12.849709 (2010).

[14] Raut, S., Petosa, A., "A compact printed bowtie antenna for ultra-wideband applications," Proceedings of European Microwave Conference, 081-084 (2009).

[15] Soumekh, M., [synthetic aperture radar signal processing], John Wiley and Sons, 1999.

[16] Dogaru, T., Nguyen, L., Le, C., “Computer models of the human body signature for sensing through the wall radar applications,” Army Research Lab ARL-TR-4290, (2007).

[17] Chan, B. H., Sévigny, P., DiFilippo, D. J., “Free space target signatures and analysis of discriminants for human targets for the 3-D L-band through-wall experimental SAR system,”, Defence Research & Development Canada – Ottawa TM 2012-182, (2012).

[18] McGill, R., Tukey, J. W., and Larsen, W. A., “Variations of Boxplots,” The American Statistician, 32(1), 12-16, (1978).

[19] Adams, R., Bischof, L., “Seeded region growing,” IEEE Transactions of Pattern Analysis and Machine Intelligence, 16(6), 641-647, (1994).

[20] Chan, B., Sévigny, P., DiFilippo, D. J., “Analysis of discriminants for experimental 3-D SAR imagery of human targets”, Proceedings of SPIE 9244, 9244-59 (2014).

Annex A 2012 trial targets

The 3-D free space and through-wall data used in this report, acquired during the 2012 Trials, are listed in Table A.1 along with the target description.

Table A.1: *List of scenes and associated targets used in this report.*

Scene identifier	Scene filename	Human target description
3	ts_front_s3_01	H2 – standing in free space on gravel
		H3 – standing in free space on gravel
		H6 – standing arms stretched in free space on gravel
4	ts_front_s4_01	H2 – standing arms stretched in free space on gravel
		H6 – kneeling in free space on gravel
6	ts_front_s5_02	H2 – holding AK47 at an angle in free space on gravel
		H3 – holding AK47 vertically in free space on gravel
8	ts_front_s6_03	H6 – sitting on chair in free space on gravel H2 – holding AK47 at an angle in free space on gravel H3 – holding AK47 vertically in free space on gravel
9	ts_front_s6_03	H1 – standing in free space on gravel
		H4 – standing in free space on gravel
		H5 – standing in free space on gravel
		Empty chair in free space on gravel
10	ts_front_s7_02	H1 – standing in free space on gravel
		H4 – standing in free space on gravel
128	502_fs_s1_01	H1 – standing in free space on asphalt
		H7 – standing in free space on asphalt
		H8 – standing in free space on asphalt
		H9 – standing in free space on asphalt
		H10 – standing in free space on asphalt
129	502_fs_s2_01	H6 – standing in free space on asphalt
		H11 – standing in free space on asphalt
		H12 – standing in free space on asphalt
11	ts_back_s8_04	H1 – standing behind drywall
12	ts_back_s9_02	H1 – kneeling behind drywall
14	ts_back_s11_01	H1 – holding AK-47 vertically behind drywall
15	ts_back_s12_01	H1 – holding AK-47 at an angle behind drywall
92	bar_hmid_01	H1 – standing behind cinder block wall
95	bar_hmid_s2_01	H1- standing arms stretched behind cinder block wall
108	bar_hmid_s8_01	H1 – sitting on chair behind cinder block wall
109	bar_hmid_s9_01	Empty chair behind cinder block wall
113	bar_hmid_s13_01	H1 – holding AK-47 vertically behind cinder block wall
114	bar_hmid_s15_02	H1 – holding AK-47 at an angle behind cinder block wall
115	bar_hmid_s15_02	H1 – kneeling behind cinder block wall
125	502_hfar_01	H1 – standing behind brick/cinder block wall
126	502_hfar_s1_02	H1 – holding AK-47 vertically behind brick/cinder block wall
127	502_hfar_s2_01	H1 – holding AK-47 at an angle behind brick/cinder block wall

This page intentionally left blank.

Annex B Human standing target signatures

The top, front, and side view 2-D slices at the PMI of the 3-D SAR data of all human standing targets in free space are shown in Figure B.1.

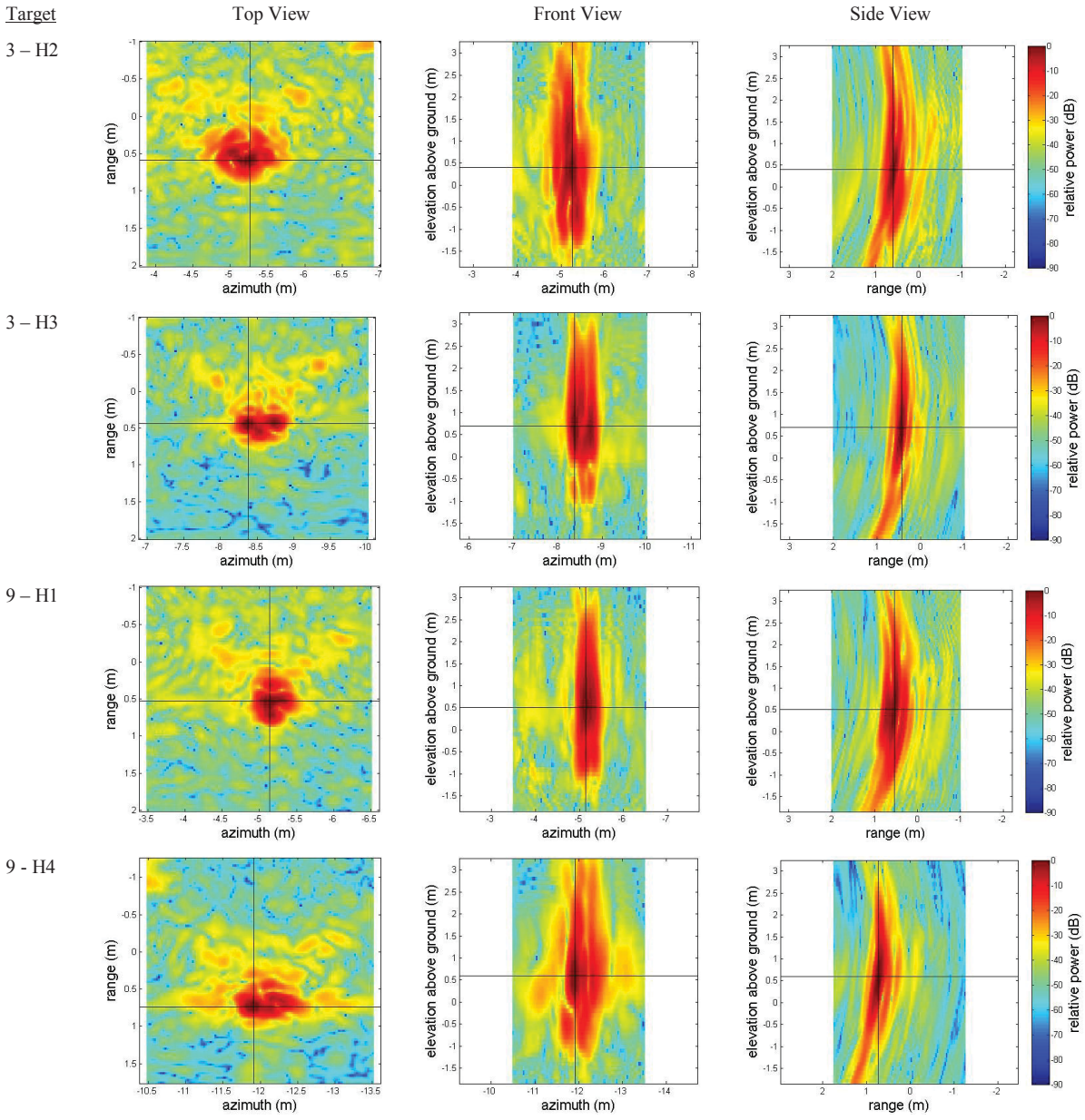

9 – H5

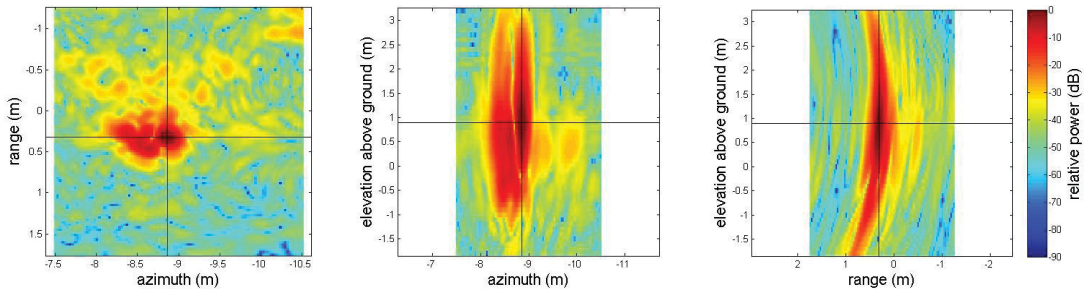

10 – H1

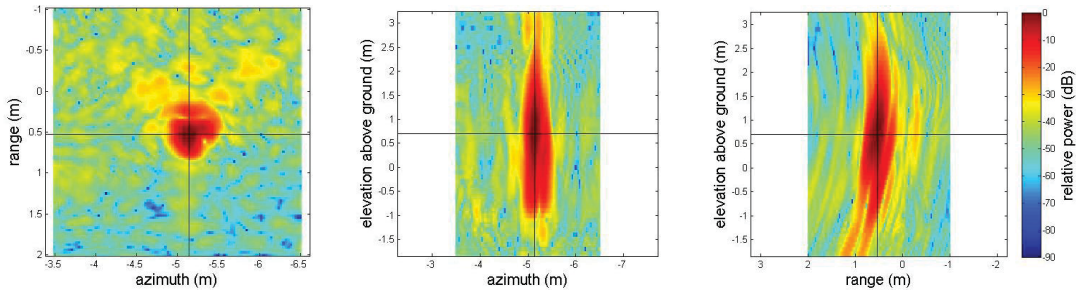

10 – H4

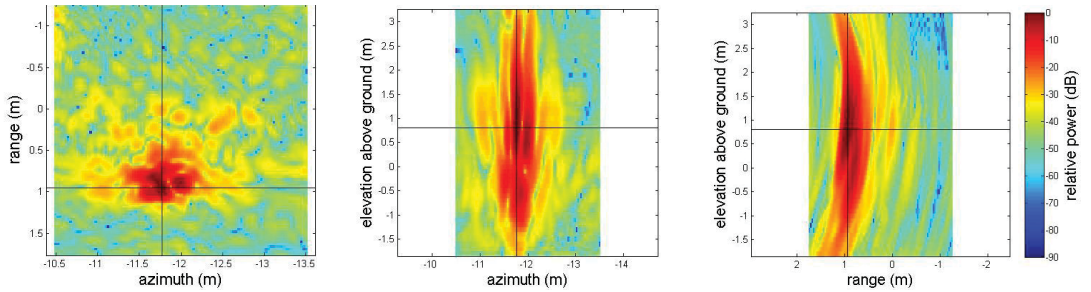

128 – H1

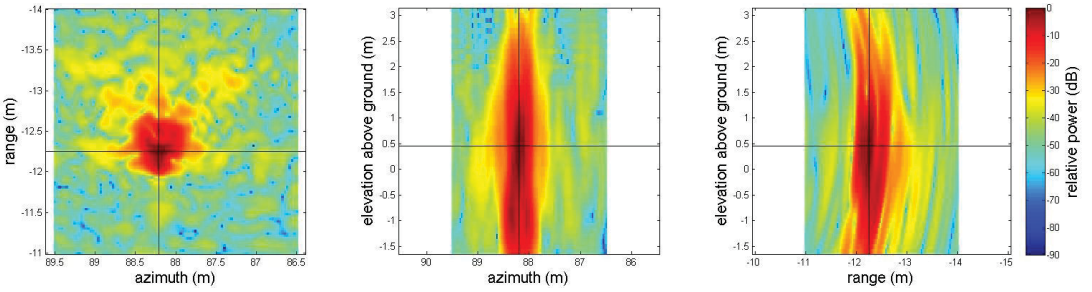

128 – H7

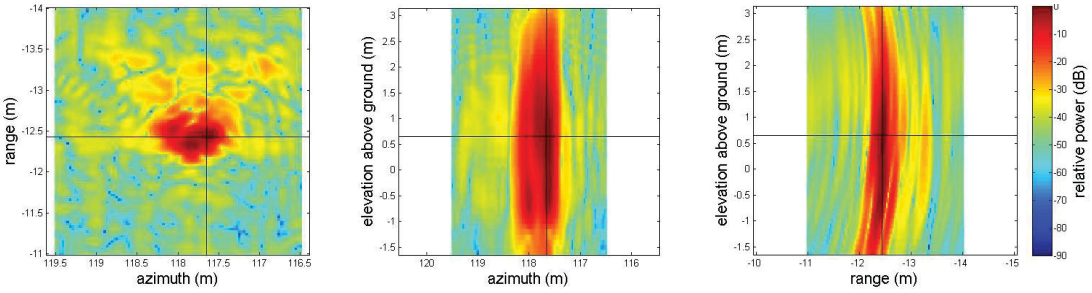

128 – H8

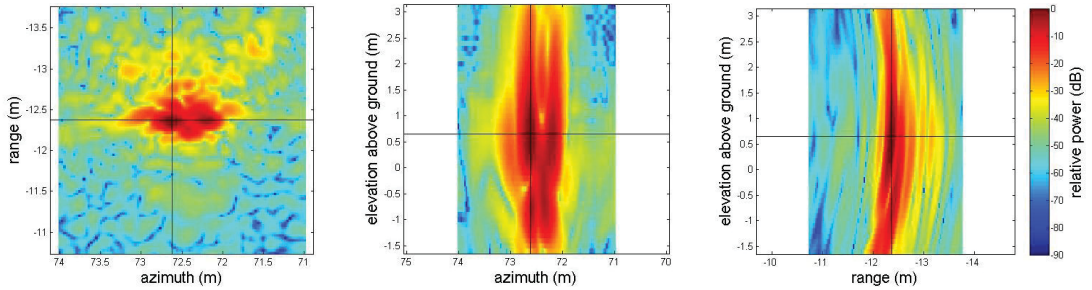

128 – H9

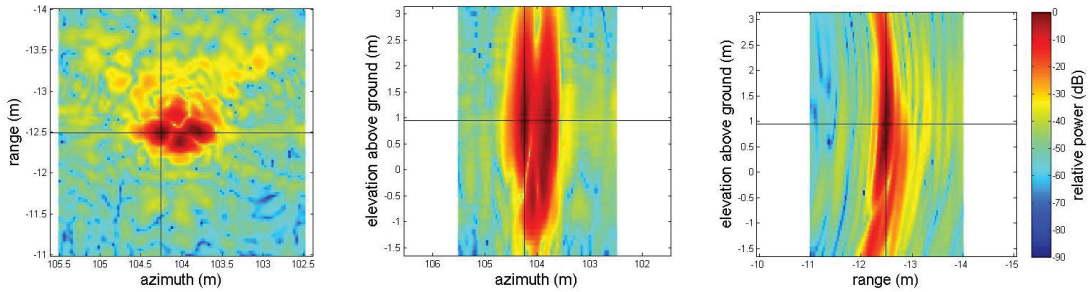

128 – H10

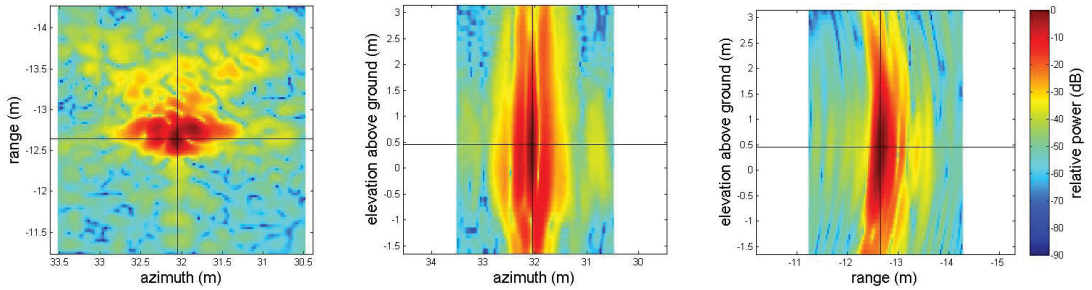

129 – H6

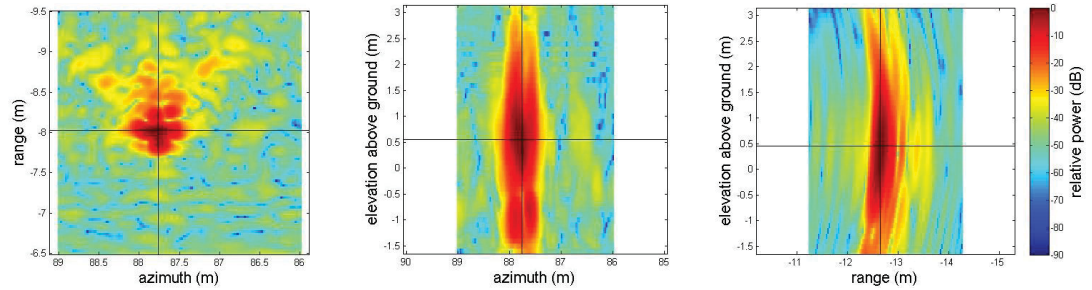

129 – H11

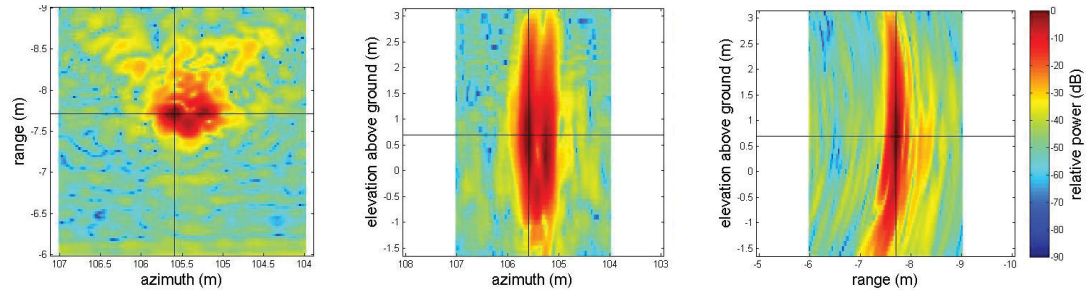

129 –
H12

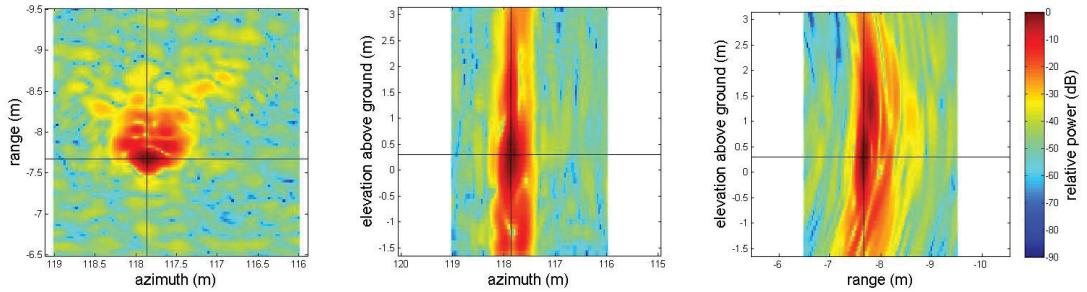

Figure B.1*: Top, front, and side view 2-D slices at the PMI of 3-D SAR data of all human standing targets in free space.*

DOCUMENT CONTROL DATA

(Security markings for the title, abstract and indexing annotation must be entered when the document is Classified or Designated)

1. ORIGINATOR (The name and address of the organization preparing the document. Organizations for whom the document was prepared, e.g., Centre sponsoring a contractor's report, or tasking agency, are entered in Section 8.)

DRDC – Ottawa Research Centre
Defence Research and Development Canada
3701 Carling Avenue
Ottawa, Ontario K1A 0Z4
Canada

2a. SECURITY MARKING (Overall security marking of the document including special supplemental markings if applicable.)

UNCLASSIFIED

2b. CONTROLLED GOODS

(NON-CONTROLLED GOODS)
DMC A
REVIEW: GCEC APRIL 2011

3. TITLE (The complete document title as indicated on the title page. Its classification should be indicated by the appropriate abbreviation (S, C or U) in parentheses after the title.)

Analysis of metrics for human detection behind walls using experimental 3-D synthetic aperture radar imagery

4. AUTHORS (last name, followed by initials – ranks, titles, etc., not to be used)

Chan, B.; Sévigny, P.; DiFilippo, D.J.

5. DATE OF PUBLICATION (Month and year of publication of document.)

December 2014

6a. NO. OF PAGES (Total containing information, including Annexes, Appendices, etc.)

52

6b. NO. OF REFS (Total cited in document.)

20

7. DESCRIPTIVE NOTES (The category of the document, e.g., technical report, technical note or memorandum. If appropriate, enter the type of report, e.g., interim, progress, summary, annual or final. Give the inclusive dates when a specific reporting period is covered.)

Scientific Report

8. SPONSORING ACTIVITY (The name of the department project office or laboratory sponsoring the research and development – include address.)

DRDC – Ottawa Research Centre
Defence Research and Development Canada
3701 Carling Avenue
Ottawa, Ontario K1A 0Z4
Canada

9a. PROJECT OR GRANT NO. (If appropriate, the applicable research and development project or grant number under which the document was written. Please specify whether project or grant.)

9b. CONTRACT NO. (If appropriate, the applicable number under which the document was written.)

10a. ORIGINATOR'S DOCUMENT NUMBER (The official document number by which the document is identified by the originating activity. This number must be unique to this document.)

DRDC-RDDC-2014-R140

10b. OTHER DOCUMENT NO(s). (Any other numbers which may be assigned this document either by the originator or by the sponsor.)

11. DOCUMENT AVAILABILITY (Any limitations on further dissemination of the document, other than those imposed by security classification.)

Unlimited

12. DOCUMENT ANNOUNCEMENT (Any limitation to the bibliographic announcement of this document. This will normally correspond to the Document Availability (11). However, where further distribution (beyond the audience specified in (11) is possible, a wider announcement audience may be selected.))

Unlimited

13. ABSTRACT (A brief and factual summary of the document. It may also appear elsewhere in the body of the document itself. It is highly desirable that the abstract of classified documents be unclassified. Each paragraph of the abstract shall begin with an indication of the security classification of the information in the paragraph (unless the document itself is unclassified) represented as (S), (C), (R), or (U). It is not necessary to include here abstracts in both official languages unless the text is bilingual.)

Defence Research & Development Canada has been investigating 3-D through wall synthetic aperture radar (SAR) imaging from an experimental L-band through-wall SAR prototype. Tools and algorithms are being developed to exploit the resulting 3-D imagery. In this report, a comprehensive study of the characteristics of human target signatures behind three different wall structures is presented using 3-D SAR data. An analysis of the human target signature in different poses behind a drywall, a cinder block wall, and a brick/cinder block wall is provided. The aim of this investigation is to determine different quantitative features that could be used as potential discriminants. A comprehensive study of 3-D human target signature metrics behind drywall is also provided. The aim of this study is to identify features for discrimination of the human target from other similar features in an empty scene including the wall signature, potential ghosts, and clutter and multipath. Several metrics were investigated as potential discriminants and six were identified as good candidates. Based on this study, no single metric could be used to fully discriminate the human targets from all others. A combination of at least three different metrics is required to achieve this. These metrics can now be implemented in an automatic human target detection algorithm for analysis.

14. KEYWORDS, DESCRIPTORS or IDENTIFIERS (Technically meaningful terms or short phrases that characterize a document and could be helpful in cataloguing the document. They should be selected so that no security classification is required. Identifiers, such as equipment model designation, trade name, military project code name, geographic location may also be included. If possible keywords should be selected from a published thesaurus, e.g., Thesaurus of Engineering and Scientific Terms (TEST) and that thesaurus identified. If it is not possible to select indexing terms which are Unclassified, the classification of each should be indicated as with the title.)

3-D SAR, imagery, through-wall, human discrimination, detection, metrics